BIOCHEMISTRY
including biophysical chemistry & molecular biology

Article

pubs.acs.org/biochemistry

Exploring the Molecular Linkage of Protein Stability Traits for Enzyme Optimization by Iterative Truncation and Evolution

Janina Speck,[†,‡] Jochen Hecky,[†,#] Heng-Keat Tam,[§,∥] Katja M. Arndt,[†,‡,⊥,@] Oliver Einsle,[§,∥,⊥,@] and Kristian M. Müller*[,†,‡,⊥]

[‡]Institute for Biochemistry and Biology, University of Potsdam, Potsdam, Germany
[†]Institute for Biology III, University of Freiburg, Freiburg im Breisgau, Germany
[§]Institute of Organic Chemistry and Biochemistry, University of Freiburg, Freiburg im Breisgau, Germany
[∥]Spemann Graduate School of Biology and Medicine (SGBM), University of Freiburg, Freiburg im Breisgau, Germany
[⊥]Centre for Biological Signalling Studies (BIOSS), University of Freiburg, Freiburg im Breisgau, Germany
[@]Freiburg Institute for Advanced Studies, University of Freiburg, Freiburg im Breisgau, Germany

Supporting Information

ABSTRACT: The stability of proteins is paramount for their therapeutic and industrial use and, thus, is a major task for protein engineering. Several types of chemical and physical stabilities are desired, and discussion revolves around whether each stability trait needs to be addressed separately and how specific and compatible stabilizing mutations act. We demonstrate a stepwise perturbation−compensation strategy, which identifies mutations rescuing the activity of a truncated TEM β-lactamase. Analyses relating structural stress with the external stresses of heat, denaturants, and proteases reveal our second-site suppressors as general stability centers that also improve the full-length enzyme. A library of lactamase variants truncated by 15 N-terminal and three C-terminal residues (Bla-NΔ15CΔ3) was subjected to activity selection and DNA shuffling. The resulting clone with the best in vivo performance harbored eight mutations, surpassed the full-length wild-type protein by 5.3 °C in T_m, displayed significantly higher catalytic activity at elevated temperatures, and showed delayed guanidine-induced denaturation. The crystal structure of this mutant was determined and provided insights into its stability determinants. Stepwise reconstitution of the N- and C-termini increased its thermal, denaturant, and proteolytic resistance successively, leading to a full-length enzyme with a T_m increased by 15.3 °C and a half-denaturation concentration shifted from 0.53 to 1.75 M guanidinium relative to that of the wild type. These improvements demonstrate that iterative truncation−optimization cycles can exploit stability−trait linkages in proteins and are exceptionally suited for the creation of progressively stabilized variants and/or downsized proteins without the need for detailed structural or mechanistic information.

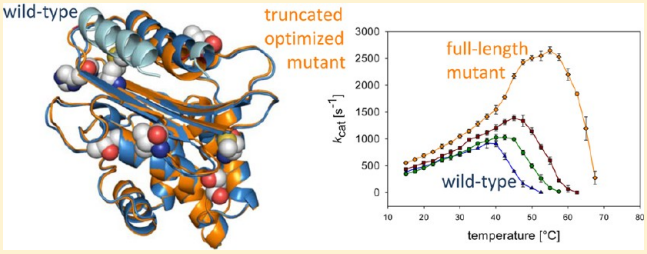

The generation of tailored proteins, particularly enzymes, is of considerable interest in making industrial processes more sustainable and cost-effective and in improving the efficacy and safety of biopharmaceuticals. However, most of the candidates featuring a desired catalytic or binding activity need to be significantly improved to satisfy the demands and standards applied to industrial and pharmaceutical products, an issue that to date has been addressed by protein engineering based on rational design and/or directed evolution techniques.[1,2]

Directed evolution (also termed in vitro evolution) is based on the generation of a gene library, e.g., by random mutagenesis or homologous recombination, followed by phenotypic screening or selection to accumulate the best-performing variants. Usually multiple cycles of mutagenesis and functional testing are necessary to obtain a satisfactory result. Despite good performance, variants with multiple substitutions may however contain mutations unfavorable to stability, folding, or solubility. Such disadvantageous mutations may be removed from the gene pool by in vitro recombination and wild-type backcrossing.

As most proteins are only marginally stable under physiological conditions, and as the vast majority of introduced mutations, including functionally beneficial ones, are structurally harmful, the stability of the parental protein strongly affects its adaptability.[3] This observation was further substantiated by recent in vitro and in silico evolutionary studies that demonstrated the positive effects of extra stability on mutational robustness and evolvability.[4−7] Consequently, by cushioning the detrimental effects of mutations on structure and performance, a stability surplus is expected to facilitate artificial design ventures in general and might even represent a

Received: December 18, 2011
Revised: March 27, 2012
Published: April 30, 2012

dx.doi.org/10.1021/bi2018738 | *Biochemistry* 2012, 51, 4850−4867

prerequisite, if the target protein is marginally stable. Furthermore, the thermal stability of biocatalysts is essential for performing industrial processes at elevated temperatures, which is often favorable because of higher reaction rates, a reduced risk of microbial contamination, and the potentially increased solubility of reactants or products.

Despite a growing body of knowledge and examples of protein stabilization by rational design, a simple and generally applicable set of rules for creating proteins with increased stability is still far out of reach.[8] However, the number of enzymes and other proteins successfully stabilized by computational design is continuously increasing.[9−11] Additionally, the wealth of sequence data obtained from genome analyses often provides the feasibility of consensus-based protein engineering.[12,13] This approach is based on a canonical amino acid sequence derived from a multiple-sequence alignment of closely related genes. Subsequent conversion of noncanonical residues in the target protein to consensus residues often results in improved structural stability. To avoid unfavorable substitutions, this concept was further refined by the implementation of statistical methods considering positional information,[14] by the use of structural information,[15] and by including a combinatorial dimension.[16]

Although computational design and consensus-based design have proven to be useful for the generation of several stabilized catalytic and noncatalytic proteins, complementary techniques that are more generally applicable and do not depend on detailed structural or mechanistic information are indispensable. One approach, termed *Proside* (protein stability increased by directed evolution), is based on directed evolution and links the infectivity of filamentous phages to the proteolytic resistance of the protein of interest (POI) by inserting the POI into the geneIII phage coat protein, which mediates host cell infection.[17−19]

In our previous work, we devised a directed evolution strategy for TEM β-lactamase that utilizes structural perturbations in the form of terminal truncations to drive selection of stabilizing mutations.[20] This perturbation−compensation approach (Figure 1A) should be applicable to an even broader range of target proteins and is based on the assumption that terminal segments (mainly regularly structured helices or strands) of proteins make subtle yet important contributions to conformational stability. Impairing the protein's structure and thus energetics incrementally by more extensive truncations should increase the selection pressure and is thus expected to pave the way to progressively stabilized functional proteins. Deletions can be easily constructed in parallel by polymerase chain reaction (PCR) and cloning; e.g., 5−10 truncated variants of a gene with a step of six nucleotides (two amino acids) can be created with little effort at low cost. If one has the information of a loose terminus or a multidomain structure, a deletion step of three to five amino acids can be chosen.

Stability has many facets because proteins, particularly in non-native settings, may resist diverse types of stresses, which can be internal, due to truncation, or external, due to exposure to heat, denaturants, or proteases. We call the interconnectedness of stress resistance "stability−trait linkage" and aim to understand and exploit this relationship. Because the deletion of five N-terminal residues of β-lactamase eliminates biological activity[20] and even the final C-terminal residue cannot be mutated without significant activity loss,[21] we also aimed to test whether such severe stress can be compensated by directed evolution and whether compensation would still provide a general benefit. For comparison, we truncated a trimeric protein that has its catalytic center at the cleft between two subunits, namely, chloramphenicol acetyltransferase (CAT), and performed directed evolution with antibiotic selection. In this case, we also obtained increased thermal stability upon re-elongation of the selected rescue mutant (S. C. Stebel et al., manuscript in preparation).

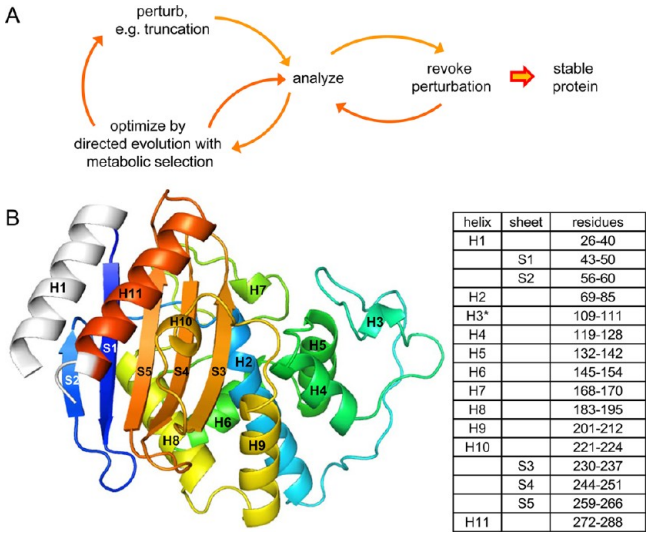

helix	sheet	residues
H1		26-40
	S1	43-50
	S2	56-60
H2		69-85
H3*		109-111
H4		119-128
H5		132-142
H6		145-154
H7		168-170
H8		183-195
H9		201-212
H10		221-224
	S3	230-237
	S4	244-251
	S5	259-266
H11		272-288

Figure 1. Work flow and protein structure. (A) Schematic representation of the perturbation−optimization work flow. The severity of the initial perturbation is chosen on the basis of the in vivo performance of various perturbed but not yet evolved variants of the protein such that a minimal residual activity is detectable. After cycles of directed evolution and optional further perturbation, the variants with rescued function are analyzed in the presence and absence of the perturbation. (B) Ribbon structure of TEM-116 β-lactamase (PDB entry 1BTL) with the indication of secondary structure elements according to Jelsch et al.[22] The corresponding residue numbers are given in the table (numbering according to Ambler et al.[34]). Residues missing in our Bla-NΔ15CΔ3 truncation variants are colored light gray. The remaining C_α trace is rainbow-colored, with blue and red indicating the N- and C-terminal portions of the polypeptide chain, respectively. The asterisk denotes that the DSSP algorithm of the WHATIF server identifies an additional helical element comprising residues 99−101 in both the 1BTL structure and the structure of our truncation mutant.

Last but not least, we wanted to test the scope of the perturbation−compensation approach and the range of the stability−trait linkage. Starting with the β-lactamase library of functional NΔ5 deletion mutants obtained in our previous study, we generated doubly truncated Bla-NΔ15CΔ3 clones and performed metabolic selection to identify stabilized, functional clones. Detailed characterizations of the best in vivo performer demonstrate how iterative truncation−optimization cycles facilitated the identification of progressively stabilized proteins.

MATERIALS AND METHODS

Wild-Type β-Lactamase Construct. As described in our previous work,[20] the β-lactamase gene (*bla*) of pUC19 served as a template for our truncation studies. Although this variant was used in several other studies[4,17,22] where it was mostly termed TEM-1 β-lactamase, it actually differs from TEM-1 by the two amino acid substitutions V84I and A184V and thus

dx.doi.org/10.1021/bi2018738 | *Biochemistry* 2012, 51, 4850−4867

equals the extended spectrum β-lactamase variant TEM-116 (http://www.lahey.org/Studies). These substitutions influence the substrate spectrum, catalytic efficiencies, and thermal stability of the enzyme.[7,23] Furthermore, to ensure comparable processing of the signal sequence and purification of impaired mutants, our constructs encode a DG dipeptide at the N-terminus and a GGHHHHH motive at the C-terminus of the proteins. These tags impose a destabilizing effect on β-lactamase, which needs to be kept in mind when comparing our data with those of other wild-type constructs. The destabilization can mainly be attributed to the DG motive (manuscript in preparation) and reduces the T_m value of the wild-type protein by 7.1 °C and that of the Bla-FL^{opt} variant by 4.4 °C (Figure S3 of the Supporting Information).

Library Construction and NExT DNA Shuffling. The generation of the Bla-NΔ15CΔ3 library was based on a library of optimized Bla-NΔ5 truncation mutants described in detail previously.[20] The β-lactamase genes of plasmids prepared from ∼2 × 10^5 Bla-NΔ5 *Escherichia coli* clones selected on agar plates containing 250−500 μg/mL ampicillin were amplified by PCR using oligonucleotides pr_Sfi-pelB-DG-shuffl and pr_GG-His5-Hind-shuffl (oligonucleotide sequences are given in Table S1 of the Supporting Information). The amplified product served as template for a PCR with oligonucleotides pr_Sfi-pelB-DG-blaNΔ15 and pr_blaCΔ3-GG-His5-Hind introducing the terminal NΔ15CΔ3 deletions. The purified PCR product was cloned via SfiI and HindIII restriction sites into vector pKJE_BlaNΔ15CΔ3_S3/6, which is a derivative of expression plasmid pAK400[24] containing an NΔ15CΔ3 version of β-lactamase variant S3/6.[20] *E. coli* XL1-Blue cells transformed with the ligation product were selected for 20 h at 37 °C on agar plates containing 25 μg/mL chloramphenicol and 150 or 300 μg/mL ampicillin. Plasmid DNA from three clones grown on agar plates with 300 μg/mL ampicillin was isolated, sequenced, and recombined by NExT DNA shuffling.[25] In brief, 5 ng of each plasmid per microliter was combined, and the mixture served as template for the PCR-based uridine incorporation using oligonucleotides pr_PAMA-DG-shuffl and pr_GG-H4-shuffl and *Taq* DNA polymerase (Genaxxon). The total concentration of dNTPs was 0.8 mM, with a U:T ratio of 1:5 (16.7% U, 83.3% T). Eight 100 μL reaction mixtures with a total amount of 7 μg of DNA were combined and concentrated to approximately 47 μL. DNA fragmentation and purification were performed as described previously.[25] A reassembly PCR was performed using 30 μL of the eluted fragments with 1.6 mM dNTPs and 5 units of *Taq* DNA polymerase in the provided buffer. The following program was used: one cycle of 94 °C for 4 min; 10 cycles of 92 °C for 30 s, 45 °C + 0.3 °C/cycle for 30 s, and 72 °C for 1 min; one cycle of 72 °C for 3 min; 15 cycles of 92 °C for 30 s, 50 °C + 0.4 °C/cycle for 30 s, and 72 °C for 1 min; one cycle of 72 °C for 3 min; 10 cycles of 92 °C for 30 s, 56 °C + 0.5 °C/cycle for 30 s, and 72 °C for 2 min; one cycle of 72 °C for 3 min; 10 cycles of 92 °C for 30 s, 61 °C + 0.5 °C/cycle for 30 s, and 72 °C for 2 min; and one cycle of 72 °C for 7 min. Ten microliters of the product was amplified by standard PCR using oligonucleotides pr_Sfi-pelB-DG-shuffl and pr_GG-His5-Hind-shuffl and *Taq* DNA polymerase. The resulting DNA was purified, cloned into the vector as described above, and transformed into *E. coli* XL1-Blue cells. The transformants were selected for ampicillin resistance at 37 °C as outlined in Results.

Signal Peptide Replacement and Reconstitution of the N- and C-Termini. Replacement of the PelB signal sequence with the BlaTEM-1 leader peptide was achieved by PCR using two forward primers, pr_ssBla-3end-DG-Bla-NΔ15-5end and pr_NdeI-ssBla-5end, and reverse primer pr_GG-His5-Hind-shuffl. Plasmid DNA encoding the corresponding lactamase variant with the PelB signal sequence served as the template. Ten microliters of the product was amplified by a second PCR using oligonucleotides pr_NdeI-ssBla-5end and pr_GG-His5-Hind-shuffl. The resulting product was cloned into vector pKJE_BlaNΔ15CΔ3_S3/6 via NdeI and HindIII restriction sites.

Reconstitution of the C-terminus was accomplished by PCR of the gene encoding truncated mutant Bla-NΔ15CΔ3^{opt} using oligonucleotides pr_XbaI-ssBla-shuffl and pr_completeCterm-His5Hind and Vent DNA polymerase. The DNA fragment was cloned into the BlaTEM-1 signal sequence containing the vector via XbaI and HindIII. The obtained pJH_BlaSS_Bla-NΔ15^{opt} construct was used to recover the N-terminal helix by PCR with oligonucleotides pr_ssBla-BlaN15recov and pr_H2-Hind-shuffl. The resulting PCR product was again amplified with the two sense primers pr_NdeI_ssBla_5end.seq and pr_ssBla-3end-Blafl-5end and antisense primer pr_H2-Hind-shuffl and cloned into vector pKJE_BlaNΔ15CΔ3_S3/6 via NdeI and HindIII restriction sites. The correctness of all constructs was confirmed by sequence analysis.

Protein Expression and Purification. Proteins were overexpressed in *E. coli* strain RV308 at 26−28 °C in an orbital shaker. Expression cultures (6−12 × 600 mL of 2×YT containing 25 μg/mL chloramphenicol) were inoculated from overnight cultures to an OD_{600} of 0.1. Overexpression was induced with 0.5 mM IPTG (isopropyl β-D-1-thiogalactopyranoside) at an OD_{600} of 0.5, and 100 μg/mL ampicillin was added 45 min after induction. Cells were harvested at an OD_{600} of 3.5−5.0 by centrifugation (10 min at 4000*g* and 4 °C). For periplasmic extraction, the cell pellet was resuspended in TES buffer [100 mM Tris, 1 mM EDTA, and 500 mM sucrose (pH 8.0)] and incubated on ice for 90 min with occasional agitation. The cell suspension was clarified by centrifugation (43000*g* for 40 min at 4 °C), and the periplasmic protein fraction was dialyzed thrice against 20 mM sodium phosphate and 500 mM sodium chloride (pH 7.0). Affinity purification of β-lactamase was performed using phenylboronate-superose affinity matrix (MoBiTec) and Ni-NTA-superflow columns (Qiagen) as described previously.[20] This two-step chromatographic purification scheme resulted in >95% pure β-lactamase as judged by Coomassie-stained 12.5% polyacrylamide gels.

Thermal Analysis by Circular Dichroism. Conformational changes were measured by monitoring the ellipticity at 222 nm as a structural probe while applying a temperature ramp from 8 to 85 °C using a spectropolarimeter (Jasco J-810) with Peltier-heated cuvette holder. Protein (10 μM) was applied in 50 mM sodium phosphate buffer (pH 7.0) using a 0.1 cm quartz cuvette, with a scan rate of 0.5 °C/min. Reverse scans (from 85 to 8 °C) revealed only partial reversibility of the thermal unfolding transition. Consequently, no rigorous thermodynamic analysis could be performed. Nevertheless, the apparent T_m values were determined according to the method of Pace et al.[26] assuming a monophasic transition. Curve fitting was performed using SigmaPlot version 11.0 (Systat Software).

Guanidinium Chloride-Induced Chemical Denaturation. Chemically induced unfolding of β-lactamase variants was investigated by analyzing samples with increasing GdmCl concentrations by circular dichroism (CD), fluorescence, and

enzyme activity measurements. For complete equilibration, the 1 mL samples [1 μM β-lactamase variant, 0−6 M GdmCl, and 50 mM sodium phosphate (pH 7.0)] were left overnight at room temperature. First, changes in tertiary structure were studied by intrinsic tryptophan fluorescence measurements using a micro quartz cuvette (HellmaAnalytics) and a spectrofluorimeter (Jasco FP-6500). The decrease in fluorescence intensity as a function of increasing GdmCl concentration was monitored at 340 nm (5 nm slit width) after excitation at 280 nm (3 and 5 nm slit widths). After fluorescence data had been acquired, samples were transferred to a CD cuvette with a 0.5 cm path length. CD spectra were recorded at 25 °C using a spectropolarimeter (Jasco J-810). Following CD analysis, the samples were diluted with the appropriate GdmCl/buffer mix in 96-well microtiter plates to a final enzyme concentration of 2 nM. A nitrocefin solution [250 μM, in 50 mM potassium phosphate and 0.5% DMSO (pH 7.0)] was added simultaneously (dilution factor of 10) to all samples of each denaturation series using a multichannel pipet, and residual enzyme activities were evaluated at 486 nm using a Tecan Sunrise plate reader. The measured fluorescence data showed a biphasic transition and were thus evaluated as described previously, using a three-state model.[20] The CD data were fit according to a monophasic transition.[26] Curve fitting was performed using SigmaPlot version 11.0 (Systat Software).

Proteinase K Challenge. The proteolytic susceptibility at 37 °C was assessed by determining changes in the CD signal at 222 nm over a period of 2 h after addition of proteinase K at a proteinase:β-lactamase ratio of 1:4. Each variant was adjusted to a final concentration of 2 μM (total volume of 1 mL in a cuvette with a 5 mm path length) and preincubated for 10 min at 37 °C. Upon addition of the proteinase, CD spectra from 260 to 190 nm were recorded every 2 min. The experimental data were fit using the three-parameter exponential decay fit implemented in SigmaPlot version 11.0 (Systat Software): $\Delta A/\Delta t = a + [(\Delta A/\Delta t)]_0 e^{-\lambda t}$, where a accounts for the residual optical activity and $t_{1/2} = \ln 2/\lambda$. For the wild-type protein and the truncated mutants, a residual signal of approximately 20% was observed. This was most likely due to the remaining peptide oligomers not cleaved by the protease. Because of the slow degradation of Bla-FL^{opt}, a was set to the average value obtained from the fits of the other three measurements to ensure consistent treatment.

Enzyme Kinetics. k_{cat} values were determined by monitoring the hydrolysis of the chromogenic cephalosporin derivative nitrocefin over time spectrophotometrically at 486 nm (Jasco V-550 spectrophotometer). For each measurement, 980 μL of a 0.2 mM nitrocefin solution [50 mM potassium phosphate and 0.5% DMSO (pH 7.0)] and 50 μL of a freshly prepared 50 nM enzyme solution were equilibrated for 5 min at the assay temperature. When 20 μL of the enzyme solution was mixed with the substrate, the change in absorption was recorded for 60 s and the maximal reaction rate was used to calculate apparent k_{cat} values using for the change in the extinction coefficient from nonhydolyzed to hydrolyzed nitrocefin at 486 nm ($\Delta\varepsilon_{486}$) a value of 16000 M^{-1} cm^{-1}. Note that assuming Michaelis−Menten kinetics [$v = v_{max} \times [S]/(K_M + [S])$] and a K_M of 50 μM, the chosen common nitrocefin concentration (0.2 mM) would give an apparent k_{cat} value that is 80% of the theoretical value. Measurements were performed in triplicate, and the standard deviation is given.

Antibiotic Resistance Tests. Precultures of transformed *E. coli* RV308 cells were grown overnight at 37 °C in LB medium (10 g tryptone, 5 g yeast extract, 10 g NaCl) supplemented with 1% glucose and 25 μg/mL chloramphenicol. Fifteen milliliters of DYT containing 25 μg/mL chloramphenicol was inoculated with the overnight culture to an OD_{600} of 0.1. For the ampicillin resistance test, the cultures were grown at 37 °C until they reached an OD_{600} of 0.5, placed on ice, and diluted to an OD_{600} of 0.0001; 100 μL of the dilution was plated on agar plates supplemented with either 25 μg/mL chloramphenicol (control plates) or 250−1000 μg/mL ampicillin. For the sensi-disc assay, the cultures were grown for 2 h at 37 °C, placed on ice, and diluted to an OD_{600} of 0.3 in DYT. Five milliliters of the dilution was pipetted on agar plates (9.4 cm diameter) containing 15 mL of medium supplemented with 25 μg/mL chloramphenicol and incubated for 1 h at room temperature. The sensi-discs were added after removal of the fluid and an additional 1 h incubation step at room temperature. The plates were incubated overnight at 37 °C, scanned, and the area of the bacterium-free halos around the filter discs was measured using ImageJ (National Institutes of Health, Bethesda, MD).

Protein Crystallization and Structure Determination. Crystals of the optimized truncated β-lactamase variant Bla-NΔ15CΔ3^{opt} were grown within 1 day at 20 °C by the sitting-drop vapor diffusion method. Drops were prepared by mixing equal volumes of a Bla-NΔ15CΔ3^{opt} solution [6.5 mg/mL, 10 mM Tris-HCl (pH 8.0)] and the reservoir solution containing 0.2 M imidazole maleate (pH 6.0) and containing 44% (w/v) polyethylene glycol 600. Crystals were directly frozen in liquid nitrogen. Diffraction data were collected from a single crystal on a rotating anode X-ray generator (Rigaku Micromax 007HF) at a wavelength of 1.54 Å using a mar345 image plate detector (mar research). The data set was processed and scaled using XDS.[27] The data were 99.7% complete to 1.90 Å resolution [41954 unique reflections (Table 4)]. Crystals belonged to space group $P2_12_12_1$ and contained two molecules per asymmetric unit with the following cell dimensions: a = 42.0 Å, b = 47.5 Å, and c = 253.8 Å. The structure of a TEM-1 variant containing the L201P substitution (PDB entry 3CMZ)[28] was used as an initial model for molecular replacement. Structure refinement was performed with REFMAC5 up to an R value of 19.9% and an R_{free} value of 23.4%.[29] The structural figures were generated with PyMol (Schrödinger LCC/DeLano Scientific). For B factor analysis, see the legend of Figure S5 of the Supporting Information.

RESULTS

Generation of a Genetic NΔ15CΔ3 Lactamase Truncation Library. In our previous study,[20] we demonstrated (i) that the removal of only a few nonconserved terminal residues may result in significantly impaired overall protein stability, (ii) that these detrimental effects can be compensated by second-site mutations, which we identified by directed evolution techniques, and (iii) that the reversal of the deletion generates a full-length variant with significantly increased stability relative to that of the wild-type protein.

Consequently, we reasoned that the truncation−optimization−re-elongation work flow is an easily executed and highly effective strategy for generating and analyzing stabilized proteins. Here we tackle the question of whether even more stable variants can be selected from a given library by increasing the selection pressure, i.e., by increasing the severity of structural perturbation using progressive truncation. Furthermore, we analyze the interconnectedness of stability toward different types of stress and test whether this strategy allows for

the generation of functional enzyme variants lacking complete secondary structure elements such as α-helices. As a starting point, we took the truncated and selected library from our previous study (NΔ5-S3 library)[20] with approximately 2 × 10^5 members and imposed a further truncation at the genetic level. The resulting NΔ15CΔ3 lactamase library clones lacked the complete 15-residue N-terminal α-helix H1 (residues 26−40) as well as three C-terminal residues (residues 288−290, numbering of residues according to Ambler et al.,[30] numbering of secondary structure elements as shown in Figure 1B, according to Jelsch et al.[22]).

Selection of Functional NΔ15CΔ3 β-Lactamase Variants. *E. coli* XL1-Blue cells harboring the cloned Bla-NΔ15CΔ3 library were selected on agar plates containing 150 or 300 μg/mL ampicillin. Only three clones survived at 300 μg/mL ampicillin. Sequence analysis revealed that the corresponding β-lactamases (named Bla-NΔ15CΔ3 mut1−mut3) contained 7−10 amino acid substitutions compared to wild-type TEM-116 lactamase (Table 1). A single round of NExT DNA shuffling[25] was applied to recombine and further diversify the genetic information of these clones.

Table 1. Mutational Pattern of Selected β-Lactamase Variants[a]

variant	amino acid substitutions
Bla-NΔ15CΔ3 mut1	N52D/E63K/I84V/V108I/**M182T**/**A224V**/**R241H**
Bla-NΔ15CΔ3 mut2	S53N/R61H/I84V/H153R/**M182T**/**T195S**/**A224V**/A227S/I247V/**T265M**
Bla-NΔ15CΔ3 mut3	T114M/E168A/**M182T**/**A224V**/**R241H**/I247V/**T265M**
Bla-NΔ15CΔ3^{opt}	I56V/R120G/**M182T**/**T195S**/I208M/**A224V**/**R241H**/**T265M**

[a]Clones Bla-NΔ15CΔ3 mut1−mut3 were derived from the previously constructed Bla-NΔ5-S3 truncation library[20] by PCR-based introduction of the desired terminal deletions and functional selection. Clone Bla-NΔ15CΔ3^{opt} was selected after recombination of Bla-NΔ15CΔ3 mut1−mut3 by NExT DNA shuffling and further selection. Substitutions of the parental genes that were recombined are shown in bold.

The recombined clones were subjected to three successive selection rounds with increasing ampicillin concentrations (first 50 μg/mL, second 200 or 300 μg/mL, and third 300−800 μg/mL). As plasmids carried cat (chloramphenicol acetyltransferase) as resistance marker, chloramphenicol was always present. Approximately 20% of the clones plated for the third selection round survived at 300 μg/mL ampicillin; 1.5% grew at 400 μg/mL, 1.0% at 500 μg/mL, and 0.2% at 600 μg/mL. Only one clone, which contained eight amino acid changing mutations in the β-lactamase gene (Table 1), survived the highest ampicillin concentration of 800 μg/mL. A comparison of the substitutions found in the three parental genes and their most powerful descendant, named Bla-NΔ15CΔ3^{opt}, showed that three mutations (I56V, R120G, and I208M) emerged during shuffling. The two mutations (M182T and A224V) present in all three parental genes were retained in the evolved protein. Four mutations (I84V, R241H, I247V, and T265M) were present in two ancestors, increasing the likelihood of being selected, but only two of them (R241H and T265M) were found in Bla-NΔ15CΔ3^{opt}. The T195S mutation was present in only one of the three parental genes.

Leader Peptide Replacement, Successive Reconstitution of the C- and N-Termini, and Protein Purification. All mutants were selected using a PelB (pectate lyase B) signal sequence, which should guide the protein to the periplasmic space via the general secretory pathway (SEC). However, a test expression culture of Bla-NΔ15CΔ3^{opt} with subsequent fractionation and analysis showed that the majority of the well-overexpressed protein accumulated as a precursor in the pellet fraction. The same behavior had been observed with the full-length form of an evolved Bla-NΔ5 truncation mutant in our previous study. In the latter case, replacing the PelB signal sequence with the native Bla^{TEM-1} leader peptide improved the fraction of processed periplasmic enzyme as well as the in vivo performance (Figure S1 of the Supporting Information). Consequently, all biophysically characterized constructs of this work were expressed with a Bla^{TEM-1} signal sequence.

To determine the orthogonality and interplay of truncation and mutations with respect to stability, we constructed two re-elongated variants of the selected Bla-NΔ15CΔ3^{opt} enzyme. The first had one terminus reconstituted, namely the C-terminus, but still lacked the N-terminal helix and was named Bla-NΔ15^{opt}. The second variant had both N- and C-termini reconstituted and was named Bla-FL^{opt}. All proteins were produced and purified as described in Materials and Methods.

Thermal Transition Analysis and Thermal Profile of Enzyme Activity. Thermostability was assessed by circular dichroism at 222 nm. Figure 2A summarizes the data of the thermal melts, and the resulting midpoints of transition (T_m values) are listed in Table 2. The evolved Bla-NΔ15CΔ3^{opt} truncation mutant showed a significantly increased melting temperature compared to that of the wild-type protein (ΔT_m = 5.3 °C). Reconstitution of the three missing C-terminal residues further increased the T_m by 2.4 °C. The full-length form of the evolved mutant, Bla-FL^{opt}, turned out to be the most stable protein in this comparison with a T_m value of 59 °C, which is 7.6 °C above the T_m of the N-helix-free mutant

Table 2. Thermal Stabilities,[a] Enzymatic Activity Profiles,[b] and Proteolytic Resistance[c]

			optimal temp		
	T_m (°C)	k_{cat} at 25 °C (s^{-1})	k_{cat} (s^{-1})	T (°C)	proteolytic stability, half-life (min)
wild type	43.7	636 ± 58	922 ± 92	37.5	3.4
Bla-NΔ15CΔ3^{opt}	49.0	611 ± 43	1029 ± 45	42.5	3.2
Bla-NΔ15^{opt}	51.4	638 ± 17	1391 ± 49	45.0	20.0
Bla-FL^{opt}	59.0	863 ± 44	2650 ± 64	55.0	41.3

[a]The midpoint of the thermal unfolding transition (T_m) was determined by fitting the data shown in Figure 2A according to the method of Pace et al.[26] [b]The enzymatic activity was determined using the substrate nitrocefin under common but nonsaturating conditions (200 μM), and the sample standard deviation calculated from triplicate measurements is given (k_{cat} ± standard deviation). [c]Half-life values were determined by fitting the exponential decay of the data shown in Figure 4.

dx.doi.org/10.1021/bi2018738 | *Biochemistry* 2012, 51, 4850−4867

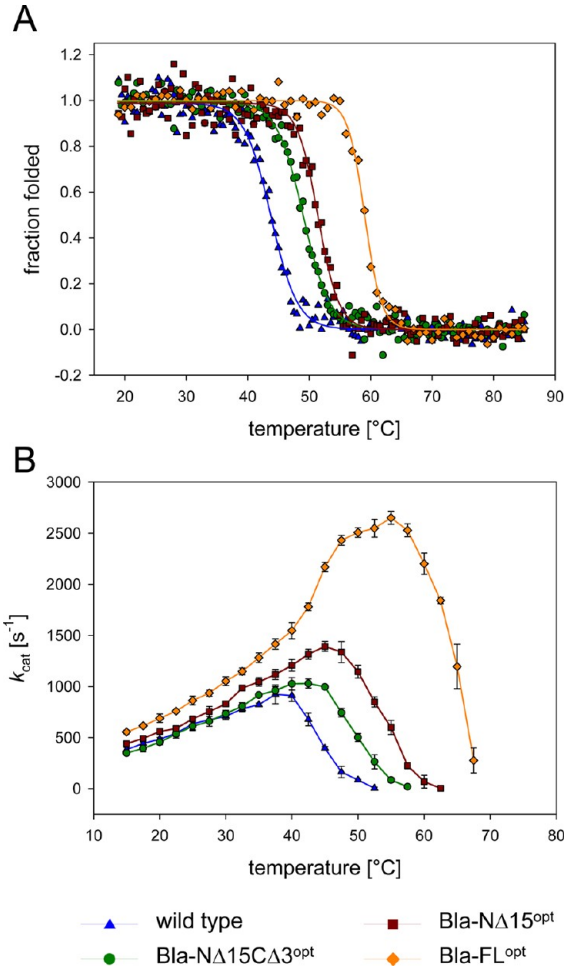

Figure 2. Temperature dependence of folding and activity of the lactamase constructs. (A) Normalized fraction folded based on CD measurements at 222 nm taken at a temperature ramp of 0.5 °C/min. Solid lines represent fits assuming a two-state transition. Relative to the wild-type construct, the evolved variants show increases in apparent T_m values of 5.3, 7.7, and 15.3 °C, respectively. (B) Catalytic rate measured with the substrate nitrocefin after a 5 min preincubation of the enzyme sample at the given temperature. Error bars give the standard deviation of triplicate measurements. The activity profiles and optimal temperatures of the mutants are shifted to higher temperatures with an overall increased k_{cat}. The analyzed proteins are the wild-type β-lactamase construct (blue triangles), the evolved variant lacking 15 N-terminal and three C-terminal residues (Bla-NΔ15CΔ3^{opt}, green circles), the evolved variant with a reconstituted C-terminus but still lacking the N-terminal helix (Bla-NΔ15^{opt}, red squares), and the evolved variant with both termini re-elongated (Bla-FL^{opt}, orange diamonds).

(Bla-NΔ15^{opt}) and 15.3 °C above the value of the wild-type construct.

The improved thermal stability of the evolved truncated as well as the reconstituted variants presumably formed the basis for the observed thermoactivity profiles, which are given in Figure 2B. At 25 °C, a temperature well below the T_m values of all four enzyme variants, the k_{cat} values were relatively similar (Table 2), with only marginal differences (<5%) among the wild type, Bla-NΔ15CΔ3^{opt}, and Bla-NΔ15^{opt}, and the k_{cat} value of Bla-FL^{opt} was ~35% above that of the wild-type protein. However, the differences became more prominent with an increase in temperature. While the wild type reached its optimal temperature at approximately 37.5 °C with a maximal k_{cat} of 922 ± 92 s^{-1}, the evolved and truncation mutant showed activity at higher temperatures with a maximal k_{cat} of 1029 ± 45 s^{-1} at 42.5 °C. The Bla-NΔ15^{opt} variant showed a maximal k_{cat} of 1391 ± 49 s^{-1} at 45 °C. For Bla-FL^{opt}, a maximal k_{cat} value of 2650 ± 64 s^{-1} was measured at 55 °C, a temperature at which the wild-type enzyme showed no residual activity at all. Overall, for each enzyme, the highest k_{cat} value was determined at an assay temperature 4–6.5 °C below the proteins' T_m values.

Thermodynamic Characterization Based on Analysis of GdmCl-Induced Unfolding. Equilibrium analysis of β-lactamase variants was performed by determining GdmCl-induced conformational changes monitored at the level of both secondary and tertiary structure using UV circular dichroism, intrinsic tryptophan fluorescence, and residual activity as structural probes. Changes in fluorescence (Figure 3A) and ellipticity (Figure 3B) as a function of denaturant concentration indicated a biphasic unfolding with a thermodynamically distinguishable intermediate, which has been postulated to be

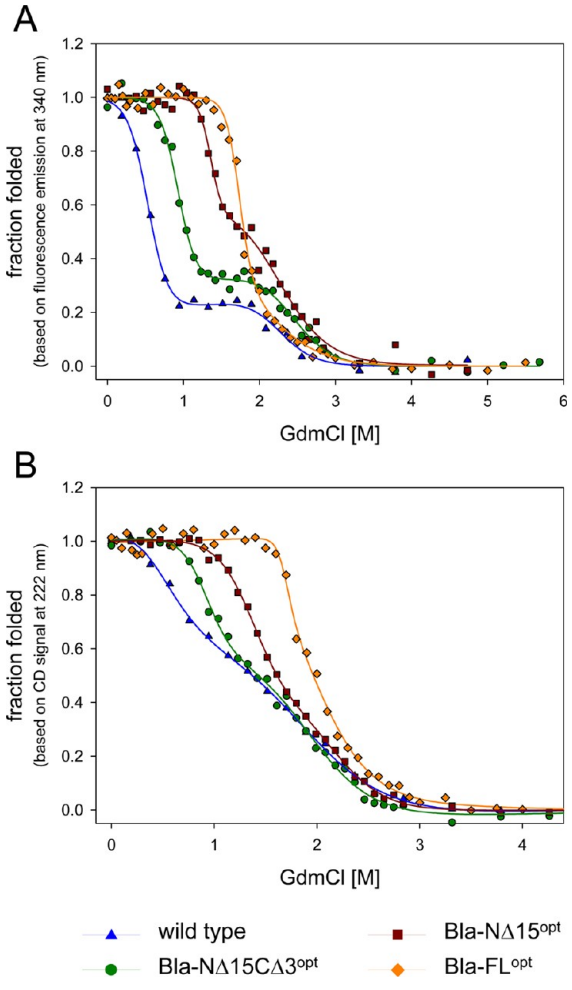

Figure 3. GdmCl-induced biphasic unfolding transitions of the lactamase constructs. (A) Intrinsic tryptophan fluorescence intensity measured in equilibrium with excitation at 280 nm and emission at 340 nm. (B) Circular dichroism at 222 nm measured in equilibrium as a function of denaturant concentration. Colored lines represent three-state fits of experimental data. The thermodynamic parameters derived from data shown in panel A are listed in Table 3. The proteins are wild-type β-lactamase (blue triangles), the evolved truncation mutants Bla-NΔ15CΔ3^{opt} (green circles) and Bla-NΔ15^{opt} (red squares), and their full-length equivalent Bla-FL^{opt} (orange diamonds).

dx.doi.org/10.1021/bi2018738 | *Biochemistry* 2012, 51, 4850–4867

Table 3. Thermodynamic Parameters[a]

	$\Delta G^{\circ}_{NI,H_2O}$ (kJ mol^{-1})	m_{NI} (kJ mol^{-1} M^{-1})	$D_{1/2NI}$ (M)	$\Delta G^{\circ}_{IU,H_2O}$ (kJ mol^{-1})	m_{IU} (kJ mol^{-1} M^{-1})	$D_{1/2IU}$ (M)
wild type	9.9 ± 1.1	18.7 ± 1.9	0.53	24.6 ± 8.7	11.0 ± 4.0	2.24
Bla-NΔ15CΔ3^{opt}	19.2 ± 2.5	20.6 ± 2.5	0.93	23.8 ± 5.5	9.9. ± 2.3	2.4
Bla-NΔ15^{opt}	43.1 ± 12.1	31.6 ± 9.1	1.36	16.7 ± 6.6	7.8 ± 2.8	2.14
Bla-FL^{opt}	45.9 ± 6.7	26.2 ± 3.8	1.75	13.8 ± 12.9	6.6 ± 3.8	2.09

[a]Thermodynamic parameters refer to GdmCl-induced unfolding transitions and were determined using the fluorescence intensity data shown in Figure 3A. Data were analyzed according to the linear extrapolation method assuming a biphasic unfolding transition as described previously.[20]

of the molten globule type.[31] Enzymatic activity was lost in the first transition upon conversion of the native to the intermediate state (Figure S2 of the Supporting Information). In principle, all constructs showed three-state behavior, albeit to varying degrees and depending on the spectroscopic method used for characterization. When unfolding was followed by monitoring the shift in tryptophan fluorescence emission maxima (data not shown), the separation in two phases was less obvious, with a more prominent transition toward the unfolded state. In contrast, the preferred evaluation of the fluorescence intensity at 340 nm clearly detected three states (Figure 3A). These differing observations of energy versus intensity indicate differing influences of the polar environment on the excited state energy level and energy relaxation during unfolding. Unfolding of the wild type, Bla-NΔ15CΔ3^{opt}, Bla-NΔ15^{opt}, and Bla-FL^{opt} started at 0.3, 0.6, 1.2, and 1.4 M GdmCl, respectively, giving rise (Table 3) to half-denaturation concentrations from the native (N) to the intermediate (I) state ($D_{1/2NI}$) of 0.53, 0.93, 1.36, and 1.75 M, respectively, for the N−I transition and 2.24, 2.40, 2.14, and 2.09 M, respectively, for the I−U transition ($D_{1/2IU}$; U, unfolded state). Both transitions were clearly separated in the case of the wild-type protein and Bla-NΔ15CΔ3^{opt}, with the intermediate "plateau" between 0.8 and 1.8 M guanidine, and 1.2 and 1.8 M guanidine, respectively. For Bla-NΔ15^{opt}, the denaturant concentration required to shift from the N state to the I state was close to that driving the I−U transition, and thus, the apparent intermediate state populated only "transiently" around 1.8 M GdmCl. For the full-length variant, Bla-FL^{opt}, the two transitions almost merged. These results suggest that the three C-terminal residues present in Bla-NΔ15^{opt} but deleted in Bla-NΔ15CΔ3^{opt} are very important for native state stability but have little impact on the structure and energetics of the intermediate and fully unfolded states.

Similar effects were seen using circular dichroism measurements (Figure 3B). Again, the wild-type protein was the least stable, whereas Bla-NΔ15CΔ3^{opt}, Bla-NΔ15^{opt}, and Bla-FL^{opt} showed successively enhanced stability toward GdmCl. Three-state behavior was most apparent for the wild type and Bla-NΔ15CΔ3^{opt} and almost completely obscured for Bla-NΔ15^{opt} and Bla-FL^{opt}. In contrast to the N−I transitions, the I−U transitions occurred at very similar GdmCl concentrations and with similar slopes for all proteins. Thus, neither the presence nor the absence of the studied terminal residues nor the evolved amino acid substitutions seemingly affected changes in helix content upon interconversion of states I and U, suggesting that the terminal helices (in the full-length protein) are largely unfolded in the intermediate.

Proteolytic Resistance. The relative protein stability was further evaluated by incubating the enzyme variants at 37 °C in the presence of proteinase K and by monitoring the structural loss using far-UV circular dichroism (Figure 4). The wild-type protein and the Bla-NΔ15CΔ3^{opt} mutant were almost equally

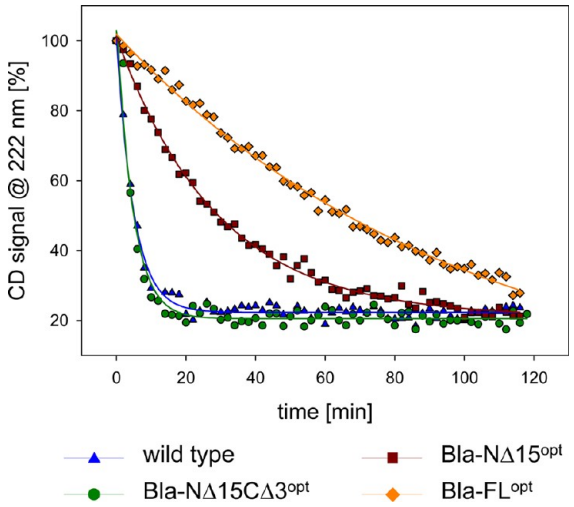

Figure 4. Proteolytic degradation rates of wild-type β-lactamase (blue triangles), the evolved truncation mutants Bla-NΔ15CΔ3^{opt} (green circles) and Bla-NΔ15^{opt} (red squares), and their full-length equivalent Bla-FL^{opt} (orange diamonds) monitored by measuring the change in circular dichroism at 222 nm upon exposure to proteinase K at 37 °C. Colored lines represent exponential decay fits of experimental data. The half-lives of Bla-NΔ15CΔ3^{opt} (3.2 min) and the wild type (3.4 min) were almost identical, whereas the re-elongated variants showed significantly increased values (20.0 min for Bla-NΔ15^{opt} and 41.3 min for Bla-FL^{opt}).

stable with calculated half-lives of 3.4 and 3.2 min, respectively (Table 2). Reconstitution of just the three C-terminal residues enhanced the resistance to proteolytic degradation significantly, shifting the half-life of the Bla-NΔ15^{opt} protein to 20.0 min. The full-length protein was again the most stable variant with a half-life of approximately 41.3 min.

Interconnectedness of in Vitro Traits. In the previous sections, we provided data about a protein scaffold subjected to four types of stress (truncation, heat, chemical denaturant, and protease treatment) while the effect was being monitored by a structural readout. In addition, we have a functional readout of the catalytic activity over a temperature range. In our setting, we prioritize the truncation and its reversal and evaluate selected mutations for their stress-counteracting properties, although we acknowledge that mutations in another context might be seen as a stress itself. A priori, there are no rules for the way in which assessed properties correlate, and indeed, every protein and mutational pattern may exhibit individual behavior. Taking the wild-type as well as the optimized truncated and the two reconstituted constructs, we plotted the values of half-denaturant concentration and half-life in the protease assay as well as the temperature of maximal catalytic activity versus the T_m value and found that there is overall a good linear correlation (Figure 5A−C). To test whether the assumption applies that a chemical reaction doubles in speed

dx.doi.org/10.1021/bi2018738 | Biochemistry 2012, 51, 4850−4867

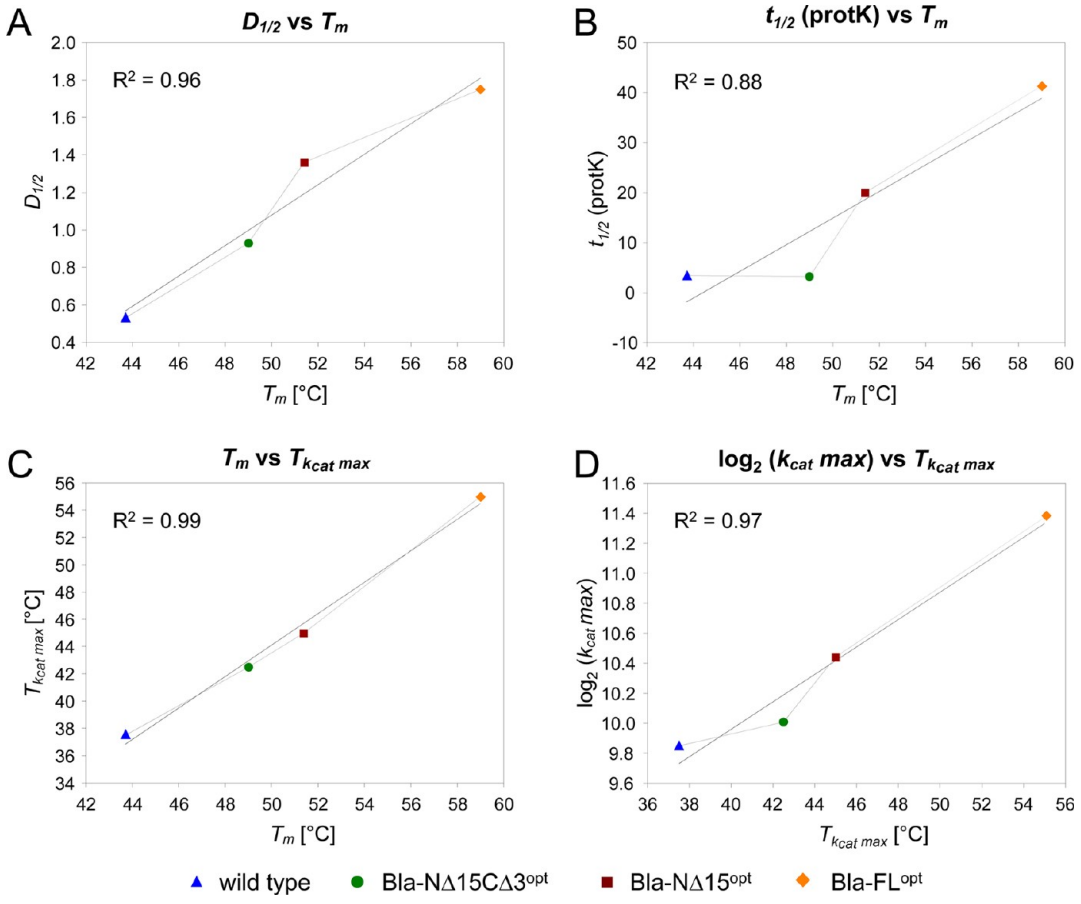

Figure 5. Correlation of traits illustrated by a linear fit between two observables. (A) Half-denaturant concentration plotted vs the melting point (T_m). (B) Half-life in the protease assay plotted vs T_m. (C) Temperature of the maximal catalytic activity plotted vs T_m. (D) Logarithm to the basis of two of the maximal catalytic activity plotted vs its temperature.

with certain temperature increases, we also plotted the logarithm to the basis of two of the k_{cat} value versus its temperature (Figure 5D). The linear fit of the logarithmic plots yields a slope of 0.0913, which translates (1/slope = ΔT) to a doubling of the reaction speed across the variants every 11 °C, indicating that the Q_{10} or van't Hoff rule can be applied. This encouraged us to take a look at the linearity of an Arrhenius-like plot [$\ln(k_{cat}\text{max})$ vs $1/T$] for the variant collection (not shown). In this case, we obtained an R factor of 0.92. The position of the data points relative to the linear regression mirrors the protease digestion (Figure 5B) and activity (Figure 5C), indicating that the wild-type construct is slightly more stable and active and that Bla-NΔ15CΔ3^{opt} is slightly less stable in comparison to the prediction that includes the two variants with the reconstituted termini.

In Vivo Performance. To evaluate the in vivo activity of the enzyme variants, we determined the relative survival of transformed bacteria on plates containing increasing concentrations of ampicillin and performed a sensi-disc assay to evaluate the substrate spectrum, including two third-generation cephalosporins.

While the Bla-NΔ15CΔ3^{opt} mutant conferred resistance to higher ampicillin concentrations than the wild-type construct, the re-elongated variants (Bla-NΔ15^{opt} and Bla-FL^{opt}) were less resistant (Figure 6A). This finding contrasts with the in vitro characterization, which clearly revealed higher stability and activity for the re-elongated variants in comparison to the wild-type enzyme as well as the truncated Bla-NΔ15CΔ3^{opt} mutant. A similar behavior was seen for the evolved Bla-NΔ5 truncation mutant S3/6 in our previous study[20] when the protein was targeted to the periplasmic space by the PelB signal sequence. Interestingly, a substitution of this SEC-targeting signal sequence by the natural Bla^{TEM-1} signal sequence as well as by leader peptides, which guide the protein to the SRP (signal recognition particle) or TAT (twin arginine translocation) pathway, led to a significant improvement in ampicillin resistance (Figure S1 of the Supporting Information). This finding taken together with the observed yield of protein purifications and the ratio of processed versus unprocessed protein in whole cell extracts indicates that the poor in vivo performance of the full-length S3/6 variant in comparison to that of the truncated version and the wild-type construct was caused by differences in the translocation efficiency. Thus, as for the re-elongated S3/6 variant, the poor in vivo activity of Bla-NΔ15^{opt} and Bla-FL^{opt} can most likely be attributed to inefficient periplasmic localization of the enzymes but not to the enzymatic function per se.

Bla-NΔ15CΔ3^{opt} was selected by survival on ampicillin-containing plates. Nonetheless, the sensi-disc assay revealed that this mutant as well as the re-elongated variants showed a substrate spectrum compared to that of the wild type (Figure 6B) at least in the same range and with an obvious trend toward broader activity, rather than a restriction to ampicillin.

Crystal Structure of the NΔ15CΔ3^{opt} β-Lactamase Variant. The crystal structure of NΔ15CΔ3^{opt} β-lactamase was determined to 1.9 Å resolution, and the details of crystallization

dx.doi.org/10.1021/bi2018738 | Biochemistry 2012, 51, 4850−4867

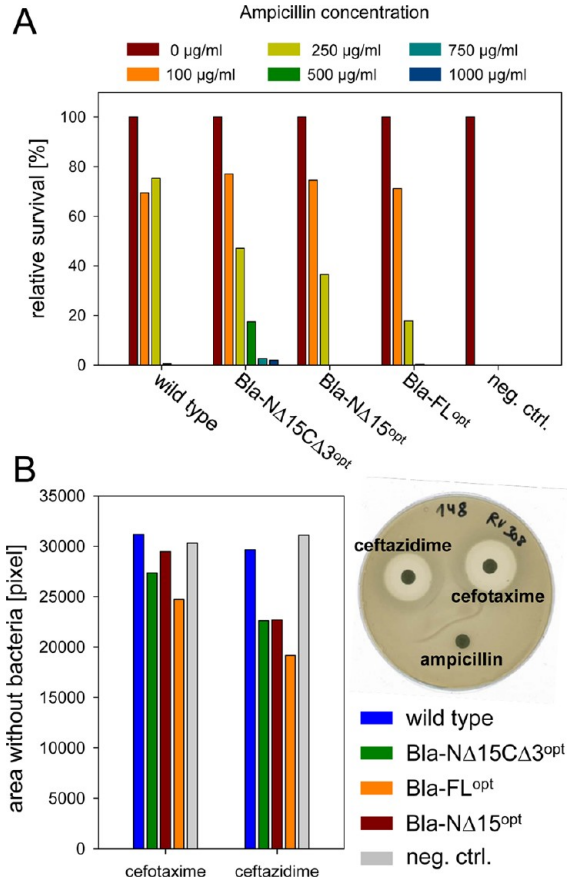

Figure 6. In vivo performance of wild-type β-lactamase and evolved mutants. (A) Relative survival of clones in the presence of different ampicillin concentrations. Plates without ampicillin served as a reference to set the 100% value. (B) Sensi-disc assay with filter disks containing 30 μg of ceftazidime, 30 μg of cefotaxime, or 10 μg of ampicillin. The area of the halo around the filter plate was evaluated to assess the relative antibiotic resistance of the clones. As an example, the plate of the Bla-NΔ15CΔ3^{opt} mutant is shown at the right. Pictures of all plates are given in Figure S4 of the Supporting Information. Bacterial cells expressing a nonfunctional β-lactamase gene, with the last 231 nucleotides truncated, served as a negative control (neg. ctrl.). Data shown were obtained with strain RV308. A comparable experiment with strain XL-1 Blue showed the same trend (data not shown).

and structure determination are summarized in Table 4 (PDB entry 3TOI). The structures of wild-type TEM-116 β-lactamase (PDB entry 1BTL)[22] and the TEM-1 L201P variant (PDB entry 3CMZ)[28] served as a reference for interpreting the consequences of amino acid substitutions. In spite of the significant structural perturbation imposed on the β-lactamase variant, the truncated and optimized protein superimposed very well with the full-length enzyme (Figure 7) with an rmsd of 0.35 Å for the positions of the backbone atoms of residues 41−271, omitting both the N-terminal (H1) and C-terminal (H11) α-helix. The only remarkable structural change regarding the backbone atoms is a significant shift of the truncated C-terminal helix H11 toward the underlying β-sheet. While the N-terminal residues of helix H11 still overlay very well with the corresponding part of the reference structure (rmsd of 0.40 Å for the backbone atoms of residues 272−274), the deviation of the C-terminus is substantial [rmsd of 1.98 Å for the backbone atoms of residues 285−287 (Figures 7 and 9A)].

Table 4. Statistics for Diffraction Data and Structure Refinement

space group	$P2_12_12_1$
cell constants *a*, *b*, *c* (Å)	42.00, 47.53, 258.83
resolution (Å)	46.74−1.90
overall completeness (%)	99.7
no. of unique reflections	41954
multiplicity (%)	6.3
$R_{merge,overall}$ (%)[a]	7.8
$R_{overall}$ (%)[b]	19.9
R_{free} (%)[c]	23.7
rmsd from ideal geometry	
bond lengths (Å)	0.007
bond angles (deg)	1.15
Φ and Ψ angle distribution (%)[d]	
most favored regions	90.3
additional allowed regions	9.2
generously allowed regions	0.5
disallowed regions	0.0

[a] $R_{merge} = \sum_{hkl}[(\sum_i|I_i - \langle I\rangle|)/\sum_i I_i]$. [b] $R = \sum_{hkl}||F_{obs}| - |F_{calc}||/\sum_{hkl}|F_{obs}|$. [c] R_{free} is the cross-validation *R* factor computed for the test set of 5% of the unique reflections. [d] Ramachandran statistics as defined by PROCHECK.

Next to the analyses of the structural effect of each mutation, which are scrutinized in Discussion, we were interested in whether we could see changes in the flexibility of the structure. Because of the influence of the crystallization conditions, the crystal packing, cocrystallized small molecules, and data processing, firm conclusions about flexibility are inherently difficult to extract from crystal structures. Nonetheless, potential trends may be inferred from plots of normalized *B* factors (Figure S5 of the Supporting Information). Overall, we detected conservation of the flexibility pattern with few minor changes. A loop region of our truncated variant around amino acids 86−88 and a region around residue 200 seem slightly less mobile compared to the nonmutated full-length structures, whereas a region around amino acids 155−168, which includes the catalytically important residue E166, and the C-terminus seem slightly more mobile. Rigidity prediction programs (e.g., KINARI)[32] calculated for the wild-type lactamase structure (PDB entry 1ZG4) a single, large rigid domain, and for the truncated, mutated lactamase (PDB entry 3TOI) the same for one molecule in the asymmetric unit and for the other molecule two rigid domains. This is in line with NMR studies reporting that wild-type TEM lactamase is one of the most rigid proteins measured by this technique.[33]

Location of Individual Mutations in the Structure. The eight mutations (Table 1) that compensated for the detrimental truncation of 18 residues were scattered across the entire molecule, equally affecting both domains (Figure 7). In the wild type, four of the mutated residues (I56, R120, T195, and R241) are surface residues (>50% solvent exposure), three (M182, I208, and A224) are partially exposed with fractional accessible surface areas of 18.5−27.5%, and only one (T265) is buried (4.7%).

Residue 56 is positioned at the edge of strand S2 and connects this outer strand to S1 by forming van der Waals contacts to I47 and V49. Residue 120 is at the N-terminal part of helix H4, where a positive charge might unfavorably interact with the helix macrodipole. M182 is at the N-cap position of helix H8, which forms part of the domain interface. In an

dx.doi.org/10.1021/bi2018738 | *Biochemistry* 2012, 51, 4850−4867

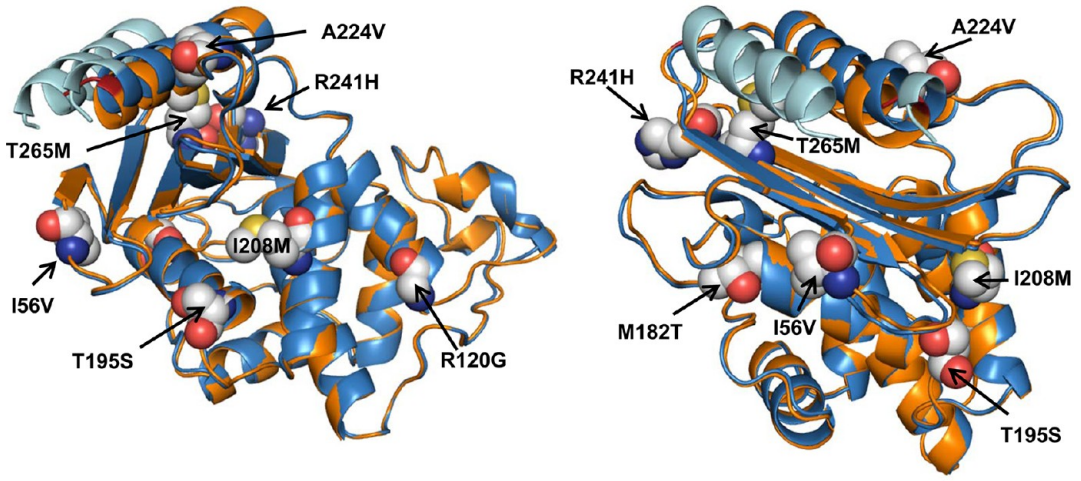

Figure 7. Superimposed ribbon structures of a full-length TEM-1 β-lactamase variant containing the L201P substitution (PDB entry 3CMZ,[28] blue) and our truncated and optimized eight-fold mutant Bla-NΔ15CΔ3^{opt} (orange). The C_α traces of both enzymes excluding terminal helices H1 and H11 superimpose very well with an rmsd of 0.35 Å, while the C-terminal helix of the mutant is significantly dislocated relative to the full-length enzyme. The residues of the full-length enzyme colored light blue correspond to the residues missing in our truncation mutant. The residues of the truncated mutant colored dark red derive from artificial tags and are not present in the wild-type protein. The side chains of the mutated amino acid residues in the Bla-NΔ15CΔ3^{opt} variant are highlighted as spheres and colored according to atom type (gray, blue, red, and yellow for carbon, nitrogen, oxygen, and sulfur atoms, respectively). The picture on the right results from a 65° rotation about the *y* axis of the structure shown on the left.

alignment of 20 class A β-lactamases, TEM-1 was the only enzyme with a methionine at this position; all others contained a threonine or serine.[34] T195 is located at the C-cap position of helix H8. Its methyl group is in van der Waals contact with L51 across the domain interface, which is removed by the T195S substitution. I208 lies in the C-terminal half of helix H9, where it forms interdomain contacts as well as contacts with M211 on the same helix and L194 from H8. A224 resides on helix H10 after the second crossover loop, where it points toward a hydrophobic surface indentation made by neighboring side chains (L221, L225, and P226) and residues from helix H11 (A280, A284, and I287) without filling it. R241 is the most exposed side chain in this set and belongs to the loop connecting S3 and S4. It most likely serves as a "solvating" residue. T265 is largely buried at the C-terminal end of strand S5. In the wild-type structure, T265 makes part of a hydrophobic core between the terminal helices and the underlying β-sheet without filling the space completely.

DISCUSSION

The generation of stabilized proteins is a fundamental task of protein engineering driven by the importance of stability for medical and industrial applications. With this work, we provide details about the scope of our previously described truncation–optimization–re-elongation strategy and demonstrate the successful application of iterative truncation–functional selection cycles to the generation of proteins with significantly improved overall stability and activity. By analyzing three structural variations (i.e., double truncation, N-terminal truncation only, and full length) with different types of external stress, we obtain a multidimensional picture of the interconnectedness of stability traits and protein structure. Remarkably, although we performed phenotypic selection at a moderate temperature (37 °C) without the addition of denaturants or proteases, we generated proteins with improved resistance toward temperature, GdmCl, and proteinase K, and an overall correlation of stability in all stress dimensions. Furthermore, the optimized enzymes not only retained their enzymatic activity at low temperatures but also showed high catalytic activity at temperatures far above the melting temperature of the wild-type protein. Importantly, the stability of the evolved protein was not obtained by enhanced rigidity at the expense of the flexibility needed for catalytic activity at low or moderate temperatures, as is the case for many naturally occurring thermophilic proteins.

Course of Selection. We used the third-generation Bla-NΔ5 truncation library described in our previous study to derive a library of Bla-NΔ15CΔ3 clones without additionally diversifying the gene pool. One selection step revealed that the Bla-NΔ5 library already contained several clones with mutations capable of compensating for the more severe structural perturbation. The three best performing clones were recombined by NExT DNA shuffling under conditions that allowed for the incorporation of additional mutations, followed by further selection to identify the best combination of mutations. The finally evolved eight-fold mutant contained three new mutations (I56V, R120G, and I208M) not present in any of the parental genes. Interestingly, the substitutions R120G and I208M were also found previously in some third-generation Bla-NΔ5 clones,[20] and they have been identified by directed evolution and metabolic selection of a circular permuted variant.[35] Furthermore, the R120G mutation was characterized as a suppressor for detrimental effects of high mutational load and increased the T_m value of TEM-116 β-lactamase by 1.8 °C.[4] The I208M substitution has also been described previously in a *Proside*-based directed evolution study with an enhancement of the T_m by 1.0 °C.[17] In contrast, a substitution of I56 with threonine instead of valine was found only once in our previous study but seemed to act neutrally. The maintenance of M182T and A224V in the evolved variant was virtually obligatory as these two mutations were already present in all sequenced third-generation Bla-NΔ5 clones on which the new library was based as well as in all three clones used for NExT DNA shuffling. Both mutations have been

dx.doi.org/10.1021/bi2018738 | *Biochemistry* 2012, 51, 4850–4867

found by others,[17,35] with M182T being probably the most frequently described global suppressor mutation in naturally occurring extended-spectrum β-lactamases (http://www.lahey.org/Studies and http://www.LacED.uni-stuttgart.de)[36] as well as in TEM β-lactamase variants derived from directed evolution.[20,37−39] According to Kather et al.,[17] M182T alone increases the T_m of TEM-116 β-lactamase by 5.7 °C, the A224V mutation by 3.1 °C, and the combination of both by 7.6 °C. The T265M mutation was also found in our previous work. From another perturbation−compensation study, where the native disulfide bridge and an important interface contact were disrupted (C77A/T71G), we know that this mutation adds 2.2 °C to the T_m of a β-lactamase that additionally contains the substitutions R120G, H153R, M182T, and A224V (manuscript in preparation). Thus, in the absence of any other suppressor mutation, the stabilizing effect of the T265M substitution on wild-type β-lactamase might be in a range similar to that of A224V, H153R, or even M182T. The absence of the H153R mutation in the evolved enzyme was surprising as this substitution occurred quite frequently (11 of 26) in the sequenced third-generation Bla-NΔ5 clones. It was shown to add 3.3 °C to the wild-type T_m value,[4] was significantly enriched in our other just mentioned study, and accumulated with increasing selection stringency in the circular permutation study.[35] Its absence in Bla-NΔ15CΔ3^{opt} might be explained by complete compensation of the perturbation by the other mutations found in Bla-NΔ15CΔ3^{opt}, as the protein has a T_m of ∼49 °C and appears to be entirely in the native form at 37 °C. Hence, the presence of the H153R mutation was not required for surviving metabolic selection at 37 °C. The same might hold true for the I247V substitution, which has also been proven to be stabilizing, although to a much lesser extent.[17] Less obvious are the contributions of the T195S and R241H substitutions with respect to stability. In another mutational context, the T195S mutation even seemed to have a negative impact on in vivo performance and thermal stability (manuscript in preparation).

Structural Role of the Deleted Terminal Residues and Their Effect on the Equilibrium Intermediate. In our previous study, we showed that truncation of wild-type β-lactamase by either five residues from the N-terminus or three residues from the C-terminus abolished the ampicillin resistance of the corresponding transformed cells when they were incubated at 37 °C. Nevertheless, it was possible to purify the N-terminally truncated protein after expression at 30 °C, and kinetic measurements at 25 °C revealed a residual activity of approximately 15% compared to that of the full-length wild-type enzyme.[20] In contrast, even at low temperatures, it was not possible to purify a NΔ15CΔ3 truncation variant of wild-type TEM-116, indicating substantial destabilization of the structural integrity of the enzyme by this more severe perturbation. In this light, the significant increase in thermal resistance achieved with a clone lacking the full N-terminal helix plus the three C-terminal residues (Bla-NΔ15CΔ3^{opt}) relative to the full-length wild-type protein was striking and demonstrated very well the suitability of iterative terminal truncation and directed evolution to produce significantly stabilized and downsized protein variants. The additional stabilization gained by restoring the three missing C-terminal residues (in Bla-NΔ15^{opt}) and the N-terminal helix (in Bla-FL^{opt}) was anticipated, yet the degree to which it affected the thermodynamics of the N−I transition was remarkable. The half-denaturation GdmCl concentration of the variant with an intact C-terminus (Bla-NΔ15^{opt}) was increased from 0.93 to 1.36 M relative to that of Bla-NΔ15CΔ3^{opt} with a concomitant increase in cooperativity and thus more than doubling of the Gibbs free energy. In summary, these changes led to almost complete convergence of the first and second transition at the level of secondary structure and very close approximation at the level of tertiary structure, indicating significant stabilization of the native state. By contrast, the I−U transition was almost unaffected by the presence or absence of C-terminal residues or by the mutations present in the evolved enzymes, indicating that the regions of all residues involved are largely unfolded in the intermediate. This is in agreement with a putative stabilization of the core within the all-α domain determined by hydrogen exchange analysis, which is centered on the disulfide bridge linking catalytic helices H2 and H4.[33] This stable α-helical assembly is most likely the last part of the protein to unfold during denaturation and should be nativelike in the intermediate state, while the termini are largely unfolded.

Truncation−Compensation Cycles and "Relevant" Stabilization of Three-State Proteins. Exclusive targeting of the native state is a crucial aspect in the stabilization of three-state proteins forming kinetic and/or equilibrium intermediates because the native state architecture ensures a functional conformation while intermediates are almost exclusively found to be inactive. Additionally, structural intermediates are often protagonists of unwanted off-pathway reactions such as aggregation and amyloidosis.[40−44] A good stabilization strategy should therefore predominantly increase the difference in free energy between the native and intermediate state (relevant stability) and not that between the intermediate and the unfolded form ("residual" stability).[45] Because of the difficulty in obtaining high-resolution structural information about intermediates, preferential stabilization of the native state to enhance the relevant stability is by no means a trivial task,[46] particularly if the intermediates involved are energetically very close to the native state.[47] We feel confident that using terminally truncated proteins as frameworks for mutagenesis and functional selection (or screening) is an excellent way to target preferentially the stability of the native state as long as the exploited selection or screening procedures can discriminate between the native state and any other state. Several folding and truncation studies indicate that residues at the chain ends often interact with more central parts of the molecule forming tertiary contacts that act as molecular clamps. The removal of such tertiary locks by careful truncation does not prevent formation of local secondary structure and hydrophobic chain collapse but hampers the establishment of the highly compact native state, leaving a molten globule-like structure. Within such a framework, it is almost certain that stabilizing interactions identified by phenotypic screening for any property that is associated with the native state will shift the N−I equilibrium toward the native conformation. Of course, in rare cases where, for example, the terminus is part of the catalytic center, truncation might inevitably obliterate function and testing of the other terminus or another structural perturbation is advised.

Structural Analysis and Interpretation of Individual Selected Mutations. The concerted action of a set of eight mutations isolated in our second truncation−evolution cycle by metabolic selection shifted the thermostability of TEM-1 β-lactamase by ∼15 °C. As seen in many other studies, these mutations are broadly distributed across the structure (Figure 7). A comparison of the structural information from full-length

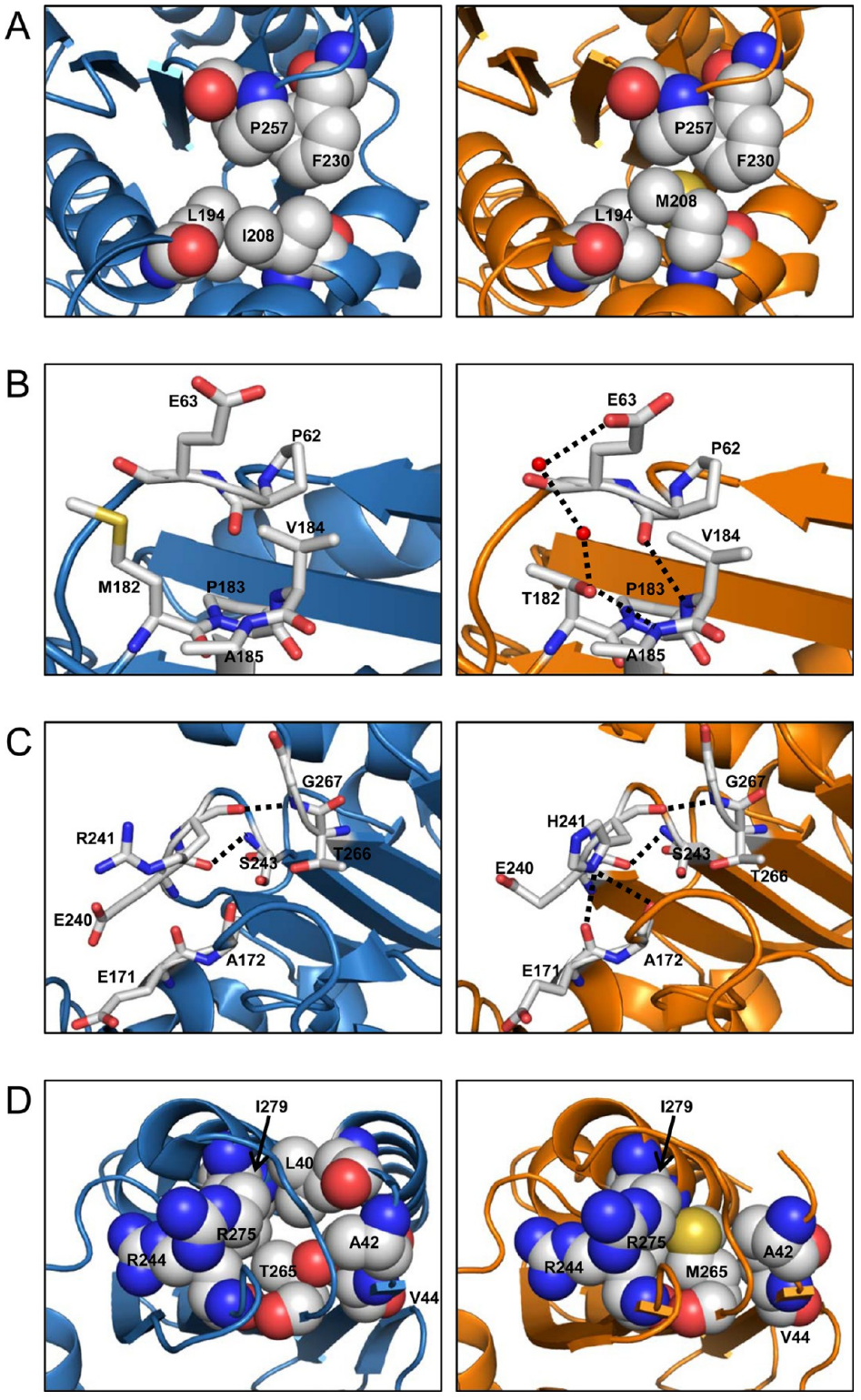

Figure 8. Comparison of the local structure in the vicinity of substitutions found in the truncated and optimized Bla-NΔ15CΔ3^{opt} variant (orange) with the corresponding region of the full-length L201P variant of TEM-1 β-lactamase (PDB entry 3CMZ, blue)[28] or, in the case of panel B, wild-type TEM-116 β-lactamase (PDB entry 1BTL, blue).[22] (A) I208M, (B) M182T, (C) R241H, and (D) T265M. The side chains of the indicated amino acid residues are shown as spheres or sticks and colored according to atom type (gray, blue, red, and yellow for carbon, nitrogen, oxygen, and sulfur atoms, respectively). Water molecules are shown as red spheres.

TEM β-lactamases from various sources with our structure of the optimized N- and C-terminally truncated mutant allowed us to draw a consistent picture of possible underlying mechanisms. According to a hydrogen exchange study, the most robust part of the structure is formed by 18 residues (75−81, 122 and 123, 138 and 139, 193 and 194, and 207−211 on helices H2, H4, H5, H8, and H9, respectively) in the immediate vicinity of the disulfide bridge connecting catalytic helices H2 and H4.[33] It has

dx.doi.org/10.1021/bi2018738 | *Biochemistry* 2012, 51, 4850−4867

been suggested that this slow exchange core is built up in an initial phase of folding[48,49] and is the last part to unfold.[33] Thus, stronger coupling of adjacent structural elements to the solid core emerges as one possible strategy for overall stabilization. It has been shown that (sub)domain interactions can play a pivotal role in stability and that autonomously folding units can serve as scaffolds for the folding of less stable parts.[50−52] In β-lactamases, the three helices H2, H8, and H9 harboring the bulk of residues forming the slow exchange core are also involved in the formation of the domain interface. One of two interface residues from helix H9 is I208. In the TEM-116 wild-type protein (PDB entry 1BTL)[22] as well as in an L201P mutant of TEM-1 β-lactamase (PDB entry 3CMZ),[28] I208 contacts L194 (H8) and weakly F230 (S3), A232 (S3), and P257 (loop between S4 and S5) without filling the hydrophobic pocket. Apparently, a methionine at this position fills the space much better (Figure 8A) and thus improves hydrophobic packing and strengthens the interdomain contact. According to its localization within the slow exchange core, it is possible that this particular mutation increases the residual stability more than the relevant stability. Nevertheless, the fact that the same mutation was also found in other directed evolution approaches,[7,17,35] including a circular permutation study with a disrupted second crossover loop, suggests that the corresponding part of the interface is highly relevant for overall stability.

The M182T mutation has been identified in naturally occurring extended-spectrum and inhibitor-resistant β-lactamase variants and acts as a "global suppressor" of proteolytic degradation, misfolding, and aggregation resulting from functionally advantageous but structurally harmful mutations.[3,53,54] Two possible mechanisms of action have been proposed on the basis of modeling studies and diverse X-ray structures. In the first scenario, the hydroxyl group of the M182T mutant forms one or two hydrogen bonds with the main chain carbonyl of residue E64 alone[55] or with E64 and E63,[37] leading to more stable domain interface contacts. In an alternative scenario, the M182T mutation stabilizes helix H8 as an N-cap residue by forming a hydrogen bond to the amide nitrogen of A185[56] and by recruiting water molecules that hydrogen bond with the side chain of E63.[3] Our structure corroborates the latter interpretation (Figure 8B) and suggests that T182 stabilizes the relatively solvent-exposed N-terminal side of the "interface helix" H8 by forming a hydrogen bond with the NH group of A185 and strengthens the hydrogen bond between the NH group of A184V and the CO group of P62. Thus, M182T keeps A184V in place, which is involved in hydrophobic packing with I47 and L49 from S1 and I56V from S2. Therefore, the combined substitutions of M182T and A184V, which is one of two amino acid exchanges distinguishing TEM-116 from TEM-1 (see Materials and Methods), stabilize not only the local environment but also the intradomain packing of the protein.

The T195S mutation is a relatively conservative exchange affecting the C-cap position of helix H8. Like that of T195, the hydroxyl group of the substituting serine forms a hydrogen bond to the backbone carbonyl of R191. In the wild-type β-lactamase, the T195 methyl group is in van der Waals contact with the side chain of L51. The T195S mutation abolishes this nonpolar contact and therefore probably destabilizes interdomain interactions. Accordingly, as part of another study, we compared two β-lactamase variants that contained either a serine or a threonine at position 195 in addition to substitutions H153R, M182T, and A224V. In this context, the T195S substitution reduced the T_m by 2.2 °C [protein without tags (manuscript in preparation)]. Furthermore, the comparison of homologous class A β-lactamases revealed clear preferences for hydrophobic residues, particularly leucine, at position 195.[34] However, in our NΔ15CΔ3^{opt} variant, the loosening of helix H8 by T195S is probably directly compensated by the improved interactions of M208 with L194 (Figure 8A).

All of the mutations described above can be related to improved domain interactions. The five remaining mutations are located at sites distant from the interface. Only one of them, R120G, is part of the all-α domain, located at the amino-terminal end of helix H4 (residues 119−128). In the wild-type β-lactamase, R120 is ∼50% solvent-exposed. At first sight, comparison of the structure of our truncation mutant containing the R120G substitution with β-lactamase structures containing an arginine at this position does not reveal certainty about the stabilizing effect of this mutation. One conceivable negative effect of the arginine side chain that could be relieved by mutation to glycine might arise from an unfavorable interaction with the helix macrodipole. In addition, the guanidinium group of R120 packs onto the nonpolar side chain of L91. This might hinder full solvation of the charged arginine moiety but may also cover the hydrophobic surface of the leucine moiety. However, the R120G mutation has been identified as a global suppressor of the highly destabilizing L76N mutation, and the mutation has been shown to increase the kinetic stability of β-lactamase during the transition from the unfolded state to the intermediate state.[4] Because of its stabilizing effect on the I−U equilibrium, the stabilizing mechanism of this mutation might not be able to be deduced from a native state structure.

The A224V mutation has already been analyzed in our previous study, where we proposed stronger hydrophobic packing by the bulkier valine side chain to a nonpolar indentation on the surface of the C-terminal helix H11. In the meantime, our assumption was confirmed by the structure of a full-length β-lactamase variant containing the A224V exchange.[17] A similar strengthening of the intradomain packing is seen in the structure of our truncated mutant, where V224 reinforces the interaction between the displaced C-terminal helix and helix H10 in which V224 is located. Hence, in the truncated protein, the A224V mutation stabilizes the remaining C-terminal helix and thus directly counteracts the assumed loosening of the C-terminus caused by the perturbation.

A hydrogen exchange study[33] implies that strands S5 and S1, together with the amino-terminal half of S2 and the carboxy half of helix H11, form the most stable part within the α/β domain, while the amino-terminal portion of H11, the C-terminal half of S2, almost all of S3, a great fraction of S4, and almost the complete helix H1 are rather dynamic with regard to the exchange of their amide protons. In TEM-1, I56 is located in a rather stable segment of S2, making interactions with I47 and L49 from S1 and A184 from H8. The I56V substitution appears to weaken the hydrophobic packing and thus to be rather destabilizing. However, this effect seems to be compensated by the presence of the A184V substitution and a conformational change in the I47 side chain as they fill the void created by the I56V substitution and thereby reinforce the hydrophobic interactions. Accordingly, it has been reported that the single A184V substitution increases the T_m value of TEM-1 β-lactamase by 1.4 °C by means of improved hydrophobic packing.[7]

dx.doi.org/10.1021/bi2018738 | Biochemistry 2012, 51, 4850−4867

The R241H substitution has been isolated previously in β-lactamase library selections, indicating its potential in stabilizing the protein.[7,57] R241 is located on a loop between S3 and S4 and forms a main chain−main chain hydrogen bond to the amide group of G267, positioned shortly after strand S5 (Figure 8C). The stabilizing effect of the conservative R241H exchange may result from the addition of a side chain−main chain hydrogen bond to the carbonyl group of either E171 or A172 on the ω-loop, which forms the base of the active site pocket.

In our previous Bla-NΔ5 truncation study,[20] the T265M mutation was present in all five sequenced second-generation clones but almost absent in the final library selected with a significantly increased ampicillin concentration, suggesting some harmful effects in terms of enzyme performance in vivo. Nevertheless, this mutation has been found in several natural isolates of extended-spectrum mutants and directed evolution experiments.[7,58] In both the wild-type β-lactamase and the reference L201P mutant, T265 is buried at the C-terminal end of strand S5 (Figure 8D), forming a side chain−main chain hydrogen bond to the carbonyl of R43 on strand S1 and main chain−main chain hydrogen bonds to R244 (S4). While the hydrogen bond to R43 is weakened in the T265M mutant, the hydrogen bonds to the main chain of R244 are slightly strengthened. However, the stabilizing effect of the T265M substitution is mainly explained by improved hydrophobic packing and intradomain stabilization of the truncated and displaced C-terminal helix H11. In the wild-type β-lactamase, the T265 methyl group is surrounded by the hydrocarbon moieties of R244 and R275 and the side chains of L40, V44, and I279. It could therefore serve as a hydrophobic "anchor" for the terminal helices H1 and H11, which pack against strands S1, S4, and S5. However, the provided space in the wild-type structure is not filled efficiently, while the large hydrophobic side chain of methionine in our truncated mutant structure fills the hydrophobic void almost perfectly.

C-Terminal Truncation and Conformational Change of the C-Terminal Helix H11. We created β-lactamase variants that lacked the complete N-terminal helix and the three C-terminal residues, K288, H289, and W290. As part of a hydrophobic cluster, W290 has been shown to be important for the folding and in vivo performance of TEM-1 β-lactamase.[59,60] Therefore, the C-terminal truncation alone would be expected to significantly impair the folding and function of the β-lactamase. Accordingly, it was not possible to purify a NΔ15CΔ3-truncated TEM-116 β-lactamase without any stabilizing mutations. In contrast, the optimized truncation mutant NΔ15CΔ3^{opt} was easily produced and purified, yielding amounts of protein significantly larger than the amount of full-length wild-type protein. The good production levels already indicated higher resistance to proteolysis in vivo and thus compensation of folding defects as well as improved overall stability.

Overlaying the structures of our optimized truncation mutant with those of full-length TEM β-lactamase variants revealed a shift of the remaining C-terminal helix toward the region of the lacking N-terminal helix as well as to the underlying β-sheet (Figures 7 and 9A). This resulted in a dense hydrophobic packing that decisively fortified the C-termini of the enzymes and thus increased the overall stability of the enzyme. As mentioned above, the T265M substitution plays a major role in keeping the helix H11 in close contact with the β-sheet. However, there are also contributions from several nonmutated residues in H11, which show conformational changes. For example, the conformational changes of the Y46 and L286 side chains result in new van der Waals contacts between Y46 and F60 and bring the hydrophobic moieties of L286 and I282 closer to the aromatic ring of Y46 (Figure 9A). Furthermore,

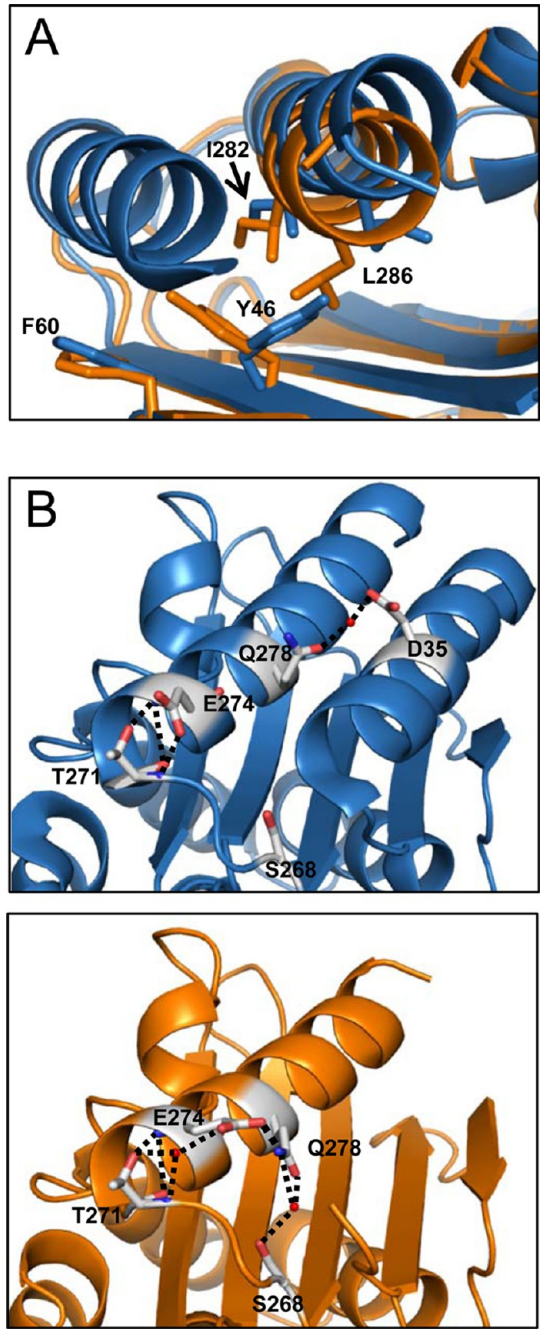

Figure 9. Conformational changes of residues of or in vicinity of the truncated C-terminal helix H11. (A) Shift of helix H11 and conformational change of Y46 and L286. (B) Conformational change of E274 and Q278 side chains and the resulting hydrogen bond network in the optimized truncation mutant Bla-NΔ15CΔ3^{opt} (orange) in comparison to the full-length L201P variant of TEM-1 β-lactamase (PDB entry 3CMZ,[25] blue). The side chains of the indicated amino acid residues are shown as sticks and colored according to atom type (gray, blue, red, and yellow for carbon, nitrogen, oxygen, and sulfur atoms, respectively). Water molecules are shown as red spheres.

dx.doi.org/10.1021/bi2018738 | Biochemistry 2012, 51, 4850−4867

E274 and Q278 are shifted toward each other and form a hydrogen bond network among E274, Q278, and S268 through a water molecule. In contrast, in the reference structure, only E274 forms a hydrogen bond with T271 while the side chain of Q278 contacts D35 on the N-terminal helix H1 through a water molecule (Figure 9B).

Catalytic Performance of Stabilized, Truncated, and Re-Elongated β-Lactamase Variants. The remarkable improvement in the stability of Bla-FL^{opt} in comparison to that of the wild-type protein was accompanied by a significant shift in the temperature optimum for catalytic activity as well as a >2.8-fold increase in the maximal catalytic activity. Also at lower temperatures, the evolved full-length enzyme exhibited reaction rates higher than that of the wild-type construct. Thus, the improved enzyme is able to function over a much broader temperature range than the wild-type protein. Despite the higher catalytic activity at 37 °C, bacteria expressing Bla-FL^{opt} showed reduced resistance to ampicillin. On the basis of our experience with another stabilized full-length protein [variant S3/6[20] (Figure S1 of the Supporting Information)], we assume that the poor in vivo performance indicates accelerated folding of the improved enzyme variants. Prior to translocation, the peptide chains of proteins that are targeted to the SEC pathway are first synthesized completely and need to be kept in a translocation compatible unfolded form. Therefore, this translocation pathway is not suited for the periplasmic targeting of proteins that exhibit premature folding.[61] In contrast, translocation by the SRP pathway occurs cotranslationally before the full peptide chain is synthesized.[62,63] This pathway is therefore more efficient for the translocation of very fast folding proteins than the SEC pathway.[64,65] For the TAT pathway, proper folding is even a prerequisite for translocation.[66,67] Thus, proteins are first synthesized, need to reach their native conformation, and are then translocated in a folded state. As would be expected for a functional, fast folding enzyme, the in vivo performance of the S3/6 full-length variant was improved by exchanging the SEC-dependent PelB signal sequence with a more efficient SEC-dependent signal sequence (Bla^{TEM-1}) or SRP- or TAT-targeting leader peptides.

On the basis of the discrepancies found between the in vitro and in vivo performance of Bla-NΔ15^{opt} and Bla-FL^{opt}, we conclude that these proteins also exhibit premature folding. In contrast to the full-length S3/6 variant, these proteins also exhibited reduced ampicillin resistance when fused to the natural Bla^{TEM-1} leader peptide, which indicates that their folding might be even more efficient. It is less likely that the translocation deficiency is the result of an impaired interaction with the protein SecB, which keeps SEC substrates in an unfolded form. As our enzymatic assays were performed with nitrocefin, we cannot rule out the possibility that Bla-FL^{opt} might have a lower activity against ampicillin; however, this would be unexpected because of the selection of the originating truncated variant for conferring better ampicillin resistance and the substrate profile seen in the sensi-disc assays.

Despite the reduced translocation efficiency, the evolved enzyme variants showed a slight increase in the resistance to at least one of the two tested third-generation cephalosporins. Such cephalosporin derivatives possess a bulky oximino side chain and are too large for the TEM-1 active site.[3] Thus, the hydrolysis of ceftazidime by our mutant indicates increased plasticity of the substrate pocket, which is also suggested by the minor increase in the *B* factors in the ω-loop. This finding again demonstrates that the improvements in stability were not based solely on the rigidification of the protein structure.

General Increase in Stability versus Local Perturbation Fix. It should be noted that our study confirms our previous observation that an imposed structural perturbation subjected to evolution based on activity selection can result in general stabilization rather than a local fix of the problem. It is remarkable to see orthogonality of stabilizing features between the deletion of a terminus and mutations at sites spread over the whole protein. Intuitively, one might have assumed that a β-sheet surface that had lost its helix cover might accumulate hydrophobic to hydrophilic changes or specifically anchor the newly exposed terminus, both of which would be a local fix of the problem. Another assumption might be that mutations providing stabilization to the truncated version are incompatible with the re-elongation to full length. In this study, only two of eight mutations (A224V and T265M) are close to the perturbation site and may directly counteract a loosening of the truncated C-terminus. Nevertheless, both mutations also contribute to the overall increase in the stability of the full-length enzyme. Thus, neither the local fix hypothesis nor the incompatibility prediction holds true in our case, even if we extend the perturbation. Our perturbation−compensation strategy allows us to conclude that stability is better accomplished with several fixes on the global scale rather than locally and that this strategy is widely applicable.

General Implications and Stability−Trait Linkage. We impose a structural stress and select for activity at 37 °C, and in return, we obtain stability at temperatures of up to 60 °C, significantly higher protease resistance, and strength against chemical denaturants. Interestingly, the T_m values of the four proteins correlated very well with the half-denaturation concentrations of their N−I transitions (R^2 = 0.96), the half-life in the protease assay (R^2 = 0.88), and the temperature of maximal catalytic activity (R^2 = 0.99). We see these results as a confirmation for our stability−trait linkage hypothesis, which states that many types of stress can be counteracted by the same molecular principles. We assume that a well-interconnected structure can withstand both the invasion of water, which is one of the main reasons for temperature-induced denaturation, and the invasion of other chemical denaturants at lower temperatures. Interconnectedness also limits the access of the proteases to the peptide chain and thus degradation. In addition, a well-interconnected structure can tolerate the removal of structural elements.

Taking a closer look at Figure 5, we can speculate whether feature versus feature plots allow one to estimate trends of the stability of the surveyed protein fold. For example, Figure 5A suggests the existence of an *x*-axis intercept, which would mean that within the set of mutated and length varied constructs a minimal thermal stability exists at which a hypothetical further destabilized protein would denature in buffer without denaturant. If we assume a linear extrapolation, the hypothetical protein of no chemical stability would still have a thermal stability of ∼37 °C and taken from Figure 5C a $T_{k_{actmax}}$ of ∼29 °C. Whether, where, and why such a chemical stability singularity exists for the given protein fold are questions in their own right requiring further study. In this study, we do not aim to make precise predictions but point to the fact that proteins that are ∼90% identical may line up with respect to their stability parameters in a certain window to warrant rough estimates of the behavior of the protein fold with or without

dx.doi.org/10.1021/bi2018738 | *Biochemistry* 2012, 51, 4850−4867

structural elements such as a full helix. Whether this is true for more mutations and length variations or for other folds has to be tested in further studies.

In general terms for stress, we can note that what you get out of directed evolution is a combination of what you engineer and select for. The simplicity of our evolutionary approach makes application to a wider range of proteins likely, including multimeric proteins and proteins of unknown structure.

■ ASSOCIATED CONTENT

Supporting Information

Photographs of *E. coli* growing on plates in the ampicillin resistance test (Figure S1), enzymatic activity of lactamase mutants in the presence of increasing concentrations of denaturant guanidinium (Figure S2), thermal denaturation followed by CD of wild-type and FL^{opt} lactamase with and without the N-terminal DG and the C-terminal GGHHHHH tags (Figure S3), sensi-disc assay (Figure S4), and an analysis of the *B* factors of our truncated lactamase mutant (PDB entry 3TOI) in comparison to PDB entries 1BTL, 1BLA, and 1ZG4 (Figure S5). This material is available free of charge via the Internet at http://pubs.acs.org.

Accession Codes

Coordinates and structure factors have been deposited in the Protein Data Bank as entry 3TOI.

■ AUTHOR INFORMATION

Corresponding Author

*Karl-Liebknecht-Str. 24-25, 14476 Potsdam, Germany. E-mail: kristian@syntbio.net. Telephone: +49-331-9775261. Fax: +49-331-9775061.

Present Address

[#]CellGenix Technologie Transfer GmbH, Freiburg, Germany.

Author Contributions

J.S. and J.H. contributed equally to this work.

Funding

This study was supported by DFG Priority Program SPP1170 and by the Excellence Initiative of the German Federal and State Governments (EXC 294, BIOSS, and GSC-4, Spemann Graduate School).

Notes

The authors declare no competing financial interest.

■ ACKNOWLEDGMENTS

We thank Prof. Andreas Plückthun for kindly providing a derivative of expression plasmid pAK400.

■ ABBREVIATIONS

Bla-NΔ15CΔ3^{opt}, evolved eight-fold β-lactamase mutant lacking 15 N-terminal and three C-terminal residues; Bla-NΔ15^{opt}, evolved eight-fold β-lactamase mutant lacking 15 N-terminal residues with a reconstituted C-terminus; Bla-FL^{opt}, full-length eight-fold β-lactamase mutant with both termini intact; NExT, Nucleotide Exchange and Excision Technology; GdmCl, guanidinium chloride; $D_{1/2}$, half-denaturation concentration; CD, circular dichroism; rmsd, root-mean-square deviation; SEC, general secretory pathway; SRP, signal recognition pathway; TAT, twin arginine translocation pathway; PDB, Protein Data Bank.

■ REFERENCES

(1) Otten, L. G., Hollmann, F., and Arends, I. W. C. E. (2010) Enzyme engineering for enantioselectivity: From trial-and-error to rational design? *Trends Biotechnol. 28*, 46−54.

(2) Turner, N. J. (2009) Directed evolution drives the next generation of biocatalysts. *Nat. Chem. Biol. 5*, 567−573.

(3) Wang, X., Minasov, G., and Shoichet, B. K. (2002) Evolution of an Antibiotic Resistance Enzyme Constrained by Stability and Activity Trade-offs. *J. Mol. Biol. 320*, 85−95.

(4) Bershtein, S., Goldin, K., and Tawfik, D. S. (2008) Intense neutral drifts yield robust and evolvable consensus proteins. *J. Mol. Biol. 379*, 1029−1044.

(5) Bloom, J. D., Labthavikul, S. T., Otey, C. R., and Arnold, F. H. (2006) Protein stability promotes evolvability. *Proc. Natl. Acad. Sci. U.S.A. 103*, 5869−5874.

(6) Bloom, J. D., Silberg, J. J., Wilke, C. O., Drummond, D. A., Adami, C., and Arnold, F. H. (2005) Thermodynamic prediction of protein neutrality. *Proc. Natl. Acad. Sci. U.S.A. 102*, 606−611.

(7) Brown, N. G., Pennington, J. M., Huang, W., Ayvaz, T., and Palzkill, T. (2010) Multiple Global Suppressors of Protein Stability Defects Facilitate the Evolution of Extended-Spectrum TEM β-Lactamases. *J. Mol. Biol. 404*, 832−846.

(8) Pantazes, R. J., Grisewood, M. J., and Maranas, C. D. (2011) Recent advances in computational protein design. *Current opinion in structural biology*, Vol. *21*, pp 467−472, Elsevier Ltd., Amsterdam.

(9) Joo, J. C., Pack, S. P., Kim, Y. H., and Yoo, Y. J. (2011) Thermostabilization of *Bacillus circulans* xylanase: Computational optimization of unstable residues based on thermal fluctuation analysis. *J. Biotechnol. 151*, 56−65.

(10) Kim, S. J., Lee, J. A., Joo, J. C., Yoo, Y. J., Kim, Y. H., and Song, B. K. (2010) The development of a thermostable CiP (*Coprinus cinereus* peroxidase) through in silico design. *Biotechnol. Prog. 26*, 1038−1046.

(11) Korkegian, A., Black, M. E., Baker, D., and Stoddard, B. L. (2005) Computational thermostabilization of an enzyme. *Science 308*, 857−860.

(12) Steipe, B., Schiller, B., Plückthun, A., and Steinbacher, S. (1994) Sequence statistics reliably predict stabilizing mutations in a protein domain. *J. Mol. Biol. 240*, 188−192.

(13) Lehmann, M., Kostrewa, D., Wyss, M., Brugger, R., D'Arcy, A., Pasamontes, L., and van Loon, A. P. (2000) From DNA sequence to improved functionality: Using protein sequence comparisons to rapidly design a thermostable consensus phytase. *Protein Eng. 13*, 49−57.

(14) Magliery, T. J., and Regan, L. (2004) Beyond consensus: Statistical free energies reveal hidden interactions in the design of a TPR motif. *J. Mol. Biol. 343*, 731−745.

(15) Polizzi, K. M., Chaparro-Riggers, J. F., Vazquez-Figueroa, E., and Bommarius, A. S. (2006) Structure-guided consensus approach to create a more thermostable penicillin G acylase. *Biotechnol. J. 1*, 531−536.

(16) Amin, N., Liu, A. D., Ramer, S., Aehle, W., Meijer, D., Metin, M., Wong, S., Gualfetti, P., and Schellenberger, V. (2004) Construction of stabilized proteins by combinatorial consensus mutagenesis. *Protein Eng., Des. Sel. 17*, 787−793.

(17) Kather, I., Jakob, R. P., Dobbek, H., and Schmid, F. X. (2008) Increased folding stability of TEM-1 β-lactamase by in vitro selection. *J. Mol. Biol. 383*, 238−251.

(18) Sieber, V., Plückthun, A., and Schmid, F. X. (1998) Selecting proteins with improved stability by a phage-based method. *Nat. Biotechnol. 16*, 955−960.

(19) Wunderlich, M., Martin, A., and Schmid, F. X. (2005) Stabilization of the cold shock protein CspB from *Bacillus subtilis* by evolutionary optimization of Coulombic interactions. *J. Mol. Biol. 347*, 1063−1076.

(20) Hecky, J., and Müller, K. M. (2005) Structural perturbation and compensation by directed evolution at physiological temperature leads to thermostabilization of β-lactamase. *Biochemistry 44*, 12640−12654.

(21) Huang, W., Petrosino, J., Hirsch, M., Shenkin, P. S., and Palzkill, T. (1996) Amino acid sequence determinants of β-lactamase structure and activity. *J. Mol. Biol. 258*, 688−703.
(22) Jelsch, C., Mourey, L., Masson, J. M., and Samama, J. P. (1993) Crystal structure of *Escherichia coli* TEM1 β-lactamase at 1.8 Å resolution. *Proteins 16*, 364−383.
(23) Chaibi, E. B., Peduzzi, J., Barthelemy, M., and Labia, R. (1997) Are TEM β-lactamases encoded by pBR322 and Bluescript plasmids enzymatically indistinguishable? *J. Antimicrob. Chemother. 39*, 668−669.
(24) Krebber, A., Bornhauser, S., Burmester, J., Honegger, A., Willuda, J., Bosshard, H. R., and Plückthun, A. (1997) Reliable cloning of functional antibody variable domains from hybridomas and spleen cell repertoires employing a reengineered phage display system. *J. Immunol. Methods 201*, 35−55.
(25) Müller, K. M., Stebel, S. C., Knall, S., Zipf, G., Bernauer, H. S., and Arndt, K. M. (2005) Nucleotide exchange and excision technology (NExT) DNA shuffling: A robust method for DNA fragmentation and directed evolution. *Nucleic Acids Res. 33*, e117.
(26) Pace, C. N., Hebert, E. J., Shaw, K. L., Schell, D., Both, V., Krajcikova, D., Sevcik, J., Wilson, K. S., Dauter, Z., Hartley, R. W., and Grimsley, G. R. (1998) Conformational stability and thermodynamics of folding of ribonucleases Sa, Sa2 and Sa3. *J. Mol. Biol. 279*, 271−286.
(27) Kabsch, W. (2010) Integration, scaling, space-group assignment and post-refinement. *Acta Crystallogr. D66*, 133−144.
(28) Marciano, D. C., Pennington, J. M., Wang, X., Wang, J., Chen, Y., Thomas, V. L., Shoichet, B. K., and Palzkill, T. (2008) Genetic and structural characterization of an L201P global suppressor substitution in TEM-1 β-lactamase. *J. Mol. Biol. 384*, 151−164.
(29) Murshudov, G. N., Skubák, P., Lebedev, A. A., Pannu, N. S., Steiner, R. A., Nicholls, R. A., Winn, M. D., Long, F., and Vagin, A. A. (2011) REFMAC5 for the refinement of macromolecular crystal structures. *Acta Crystallogr. D67*, 355−367.
(30) Ambler, R. P., Coulson, A. F., Frère, J. M., Ghuysen, J. M., Joris, B., Forsman, M., Levesque, R. C., Tiraby, G., and Waley, S. G. (1991) A standard numbering scheme for the class A β-lactamases. *Biochem. J. 276*, 269−270.
(31) Vanhove, M., Raquet, X., and Frère, J. M. (1995) Investigation of the folding pathway of the TEM-1 β-lactamase. *Proteins 22*, 110−118.
(32) Fox, N., Jagodzinski, F., Li, Y., and Streinu, I. (2011) KINARI-Web: A server for protein rigidity analysis. *Nucleic Acids Res. 39*, W177−W183.
(33) Savard, P.-Y., and Gagné, S. M. (2006) Backbone dynamics of TEM-1 determined by NMR: Evidence for a highly ordered protein. *Biochemistry 45*, 11414−11424.
(34) Ambler, R. P., Coulson, A. F., Frère, J. M., Ghuysen, J. M., Joris, B., Forsman, M., Levesque, R. C., Tiraby, G., and Waley, S. G. (1991) A standard numbering scheme for the class A β-lactamases. *Biochem. J. 276*, 269−270.
(35) Osuna, J., Pérez-Blancas, A., and Soberón, X. (2002) Improving a circularly permuted TEM-1 β-lactamase by directed evolution. *Protein Eng., Des. Sel. 15*, 463−470.
(36) Thai, Q. K., Bös, F., and Pleiss, J. (2009) The Lactamase Engineering Database: A critical survey of TEM sequences in public databases. *BMC Genomics 10*, 390.
(37) Orencia, M. C., Yoon, J. S., Ness, J. E., Stemmer, W. P., and Stevens, R. C. (2001) Predicting the emergence of antibiotic resistance by directed evolution and structural analysis. *Nat. Struct. Biol. 8*, 238−242.
(38) Stemmer, W. P. (1994) Rapid evolution of a protein in vitro by DNA shuffling. *Nature 370*, 389−391.
(39) Zaccolo, M., and Gherardi, E. (1999) The effect of high-frequency random mutagenesis on in vitro protein evolution: A study on TEM-1 β-lactamase. *J. Mol. Biol. 285*, 775−783.
(40) Wetzel, R. (1994) Mutations and off-pathway aggregation of proteins. *Trends Biotechnol. 12*, 193−198.
(41) Fink, A. L. (1998) Protein aggregation: Folding aggregates, inclusion bodies and amyloid. *Folding Des. 3*, R9−R23.
(42) Jahn, T. R., and Radford, S. E. (2005) The Yin and Yang of protein folding. *FEBS J. 272*, 5962−5970.
(43) Jahn, T. R., Parker, M. J., Homans, S. W., and Radford, S. E. (2006) Amyloid formation under physiological conditions proceeds via a native-like folding intermediate. *Nat. Struct. Mol. Biol. 13*, 195−201.
(44) Ventura, S. (2005) Sequence determinants of protein aggregation: Tools to increase protein solubility. *Microb. Cell Fact. 4*, 11.
(45) Campos, L. A., Garcia-Mira, M. M., Godoy-Ruiz, R., Sanchez-Ruiz, J. M., and Sancho, J. (2004) Do proteins always benefit from a stability increase? Relevant and residual stabilisation in a three-state protein by charge optimization. *J. Mol. Biol. 344*, 223−237.
(46) Campos, L. A., Bueno, M., Lopez-Llano, J., Jiménez, M. A., and Sancho, J. (2004) Structure of stable protein folding intermediates by equilibrium φ-analysis: The apoflavodoxin thermal intermediate. *J. Mol. Biol. 344*, 239−255.
(47) Sancho, J., Bueno, M., Campos, L. A., Fernández-Recio, J., Irún, M. P., López, J., Machicado, C., Pedroso, I., and Toja, M. (2002) The "relevant" stability of proteins with equilibrium intermediates. *TheScientificWorldJournal 2*, 1209−1215.
(48) Gervasoni, P., and Plückthun, A. (1997) Folding intermediates of β-lactamase recognized by GroEL. *FEBS Lett. 401*, 138−142.
(49) Vanhove, M., Lejeune, A., Guillaume, G., Virden, R., Pain, R. H., Schmid, F. X., and Frère, J. M. (1998) A collapsed intermediate with nonnative packing of hydrophobic residues in the folding of TEM-1 β-lactamase. *Biochemistry 37*, 1941−1950.
(50) Llinás, M., and Marqusee, S. (1998) Subdomain interactions as a determinant in the folding and stability of T4 lysozyme. *Protein Sci. 7*, 96−104.
(51) Wörn, A., and Plückthun, A. (1998) Mutual stabilization of VL and VH in single-chain antibody fragments, investigated with mutants engineered for stability. *Biochemistry 37*, 13120−13127.
(52) Martin, A., and Schmid, F. X. (2003) Evolutionary stabilization of the gene-3-protein of phage fd reveals the principles that govern the thermodynamic stability of two-domain proteins. *J. Mol. Biol. 328*, 863−875.
(53) Huang, W., and Palzkill, T. (1997) A natural polymorphism in β-lactamase is a global suppressor. *Proc. Natl. Acad. Sci. U.S.A. 94*, 8801−8806.
(54) Sideraki, V., Huang, W., Palzkill, T., and Gilbert, H. F. (2001) A secondary drug resistance mutation of TEM-1 β-lactamase that suppresses misfolding and aggregation. *Proc. Natl. Acad. Sci. U.S.A. 98*, 283−288.
(55) Farzaneh, S., Chaibi, E. B., Peduzzi, J., Barthelemy, M., Labia, R., Blazquez, J., and Baquero, F. (1996) Implication of Ile-69 and Thr-182 residues in kinetic characteristics of IRT-3 (TEM-32) β-lactamase. *Antimicrob. Agents Chemother. 40*, 2434−2436.
(56) Minasov, G., Wang, X., and Shoichet, B. K. (2002) An ultrahigh resolution structure of TEM-1 β-lactamase suggests a role for Glu166 as the general base in acylation. *J. Am. Chem. Soc. 124*, 5333−5340.
(57) Salverda, M. L. M., De Visser, J. A. G. M., and Barlow, M. (2010) Natural evolution of TEM-1 β-lactamase: Experimental reconstruction and clinical relevance. *FEMS Microbiol. Rev. 34*, 1015−1036.
(58) Long-McGie, J., Liu, A. D., and Schellenberger, V. (2000) Rapid in vivo evolution of a β-lactamase using phagemids. *Biotechnol. Bioeng. 68*, 121−125.
(59) Huang, W., Petrosino, J., Hirsch, M., Shenkin, P. S., and Palzkill, T. (1996) Amino acid sequence determinants of β-lactamase structure and activity. *J. Mol. Biol. 258*, 688−703.
(60) Lejeune, A., Pain, R. H., Charlier, P., Frère, J.-M., and Matagne, A. (2008) TEM-1 β-lactamase folds in a nonhierarchical manner with transient non-native interactions involving the C-terminal region. *Biochemistry 47*, 1186−1193.
(61) Debarbieux, L., and Beckwith, J. (1998) The reductive enzyme thioredoxin 1 acts as an oxidant when it is exported to the *Escherichia coli* periplasm. *Proc. Natl. Acad. Sci. U.S.A. 95*, 10751−10756.

(62) Schierle, C. F., Berkmen, M., Huber, D., Kumamoto, C., Boyd, D., and Beckwith, J. (2003) The DsbA signal sequence directs efficient, cotranslational export of passenger proteins to the *Escherichia coli* periplasm via the signal recognition particle pathway. *J. Bacteriol. 185*, 5706−5713.
(63) Koch, H.-G., Moser, M., and Müller, M. (2003) Signal recognition particle-dependent protein targeting, universal to all kingdoms of life. *Rev. Physiol., Biochem., Pharmacol. 146*, 55−94.
(64) Jonda, S., Huber-Wunderlich, M., Glockshuber, R., and Mössner, E. (1999) Complementation of DsbA deficiency with secreted thioredoxin variants reveals the crucial role of an efficient dithiol oxidant for catalyzed protein folding in the bacterial periplasm. *EMBO J. 18*, 3271−3281.
(65) Steiner, D., Forrer, P., and Plückthun, A. (2008) Efficient selection of DARPins with sub-nanomolar affinities using SRP phage display. *J. Mol. Biol. 382*, 1211−1227.
(66) Fisher, A. C., and DeLisa, M. P. (2004) A little help from my friends: Quality control of presecretory proteins in bacteria. *J. Bacteriol. 186*, 7467−7473.
(67) Berks, B. C., Sargent, F., and Palmer, T. (2000) The Tat protein export pathway. *Mol. Microbiol. 35*, 260−274.